

Supplementary Information

Dual Acting Oximes Designed for Therapeutic Decontamination of Reactive Organophosphates via Catalytic Inactivation and Acetylcholinesterase Reactivation

Jayme Cannon,^{ab} Shengzhuang Tang,^{ab} Kelly Yang,^a Racquel Harrison,^a and Seok Ki Choi^{*ab}

^aMichigan Nanotechnology Institute for Medicine and Biological Sciences, University of Michigan Medical School, Ann Arbor, Michigan 48109, United States of America

^bDepartment of Internal Medicine, University of Michigan Medical School, Ann Arbor, Michigan 48109, United States of America

*To whom correspondence should be addressed, Email: skchoi@umich.edu

Table of Contents

Materials and Analytical Methods	page S2
Synthetic Methods	page S3
Assay Methods	page S9
Figure S1. Copies of spectra (Mass, ¹ H and ³ C NMR) of oximes 2–9	page S14
Figure S2. UPLC traces of oximes 2–9	page S30
Figure S3. Overlaid UV–vis spectral traces in PAMPA assay	page S31
Figure S4. Plots of reactivation rate of hAChE-OP	page S32
Figure S5. A plot of oxime effect on hAChE activity	page S33
Figure S6. Plots of reactivation rate of eAChE-OP	page S34
Figure S7. Kinetic traces of POX inactivation at pH 8.0, 17 °C	page S35
Figure S8. Kinetic traces of POX inactivation at pH 8.0, 37 °C	page S36
Figure S9. Kinetic traces of POX inactivation at pH 10.5	page S37
Figure S10. Plots of k_{obsd} in oxime-catalyzed POX inactivation	page S38
Table S1. IC ₅₀ values of OP in AChE	page S39
References	page S40

1. Materials

All reagents were purchased from commercial suppliers and used as received. These include organophosphate pesticides paraoxon (POX, purity $\geq 90\%$), chlorpyrifos (analytical standard), malaoxon (analytical standard), omethoate (analytical standard) all from Sigma-Aldrich. Oximes including diacetylmonoxime (DAM, $\geq 98\%$) and pralidoxime chloride (2-PAM, 99%), reagents for oxime synthesis including ethyl glyoxylate (50% in toluene), hydroxylamine hydrochloride (98%), iodomethane (99%), formaldehyde (36.5–38% in water), sodium cyanobohydride (95%) were purchased from Sigma-Aldrich. Primary amines used for oxime synthesis were purchased from Sigma-Aldrich that include ethylenediamine (99%), *N,N*-diethylethylenediamine (99%), 1,3-diamino-2-propanol (95%), 1-(2-aminoethyl)pyrrolidine (98%), 3-(dimethylamino)-1-propylamine (99%), 2-(aminomethyl)imidazole dihydrochloride (97%) and (\pm) 3-amino-1,2-propanediol (97%). Solvents were used as received which include methanol, ethanol, dichloromethane, and ethyl acetate, each from Fisher Scientific.

Deuterium labeled solvents for NMR analysis were purchased from Cambridge Isotope Laboratories, Inc which include CDCl_3 (99.8 atom % D) and D_2O (99.9 atom % D), each containing tetramethylsilane (TMS; 0.03% v/v) or 3-(trimethylsilyl)propionic-2,2,3,3-*d*₄ acid sodium salt (DSS; 0.05% wt/wt), respectively.

Silica gels (200–400 mesh) for column chromatography and silica plates (250 μm thick, Merck®) for thin layer chromatography (TLC) were purchased from Silicycle or Sigma-Aldrich, respectively.

2. Analytical Methods

Synthetic oximes were fully characterized in the aspect of their structural identity and homogeneity by standard analytical methods of relevance to small molecules. These include NMR (^1H , ^{13}C) spectroscopy, high resolution mass spectrometry (HRMS), and ultrahigh performance liquid chromatography (UPLC) as reported earlier.¹

Mass Spectroscopy. Mass spectral characterization was performed using a Micromass AutoSpec Ultima Magnetic sector mass spectrometer in an electrospray ionization (ESI) mode. Exact masses were measured by high resolution mass spectrometry using a VG 70-250-S mass

spectrometer (magnetic sector) in an electron ionization (EI) mode or Agilent 6230 TOF HPLC-MS with a jet stream ESI source.

NMR Spectroscopy. NMR spectra were acquired using a standard default pulse sequence at 297.3 K in a Varian spectrometer at 500 MHz for ^1H NMR and at 100 MHz for proton-decoupled ^{13}C NMR spectra. Chemical shift (δ) values are reported in ppm relative to an internal standard either TMS or DSS preadded in the deuterated solvent ($\delta = 0.00$ ppm).

UV-vis Spectrometry. Absorption spectra for paraoxon inactivation kinetics were recorded in a Perkin Elmer Lambda 20 spectrophotometer.

Ultrahigh Performance Liquid Chromatography (UPLC). UPLC analysis was performed in a Waters Acquity System equipped with a BEH C₁₈ column (100 × 2.1 mm, 1.7 μm) and integrated with a photodiode array (PDA) detector at 215 nm and 275 nm. In typical UPLC runs, each sample solution prepared at 0.2–0.5 mg/mL was injected at a volume of 3 μL and eluted at a flow rate of 0.2 mL min⁻¹. The elution involved a linear gradient composed of two mobile solvents, 0.1% (v/v) TFA in water (eluent A) and 0.1% (v/v) TFA in acetonitrile (eluent B). The mobile phase began at 1% B (0–2.0 min), linearly increased to 80% B (2.0–13.4 min) and decreased to 50% B (13.4–13.8 min) prior to going back to 1% B (13.8–14.4 min) followed by an isocratic elution at 1% B (18 min). Compound detection occurred primarily at 210 nm and 285 nm.

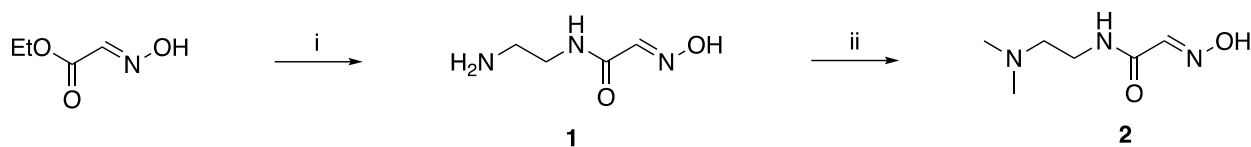
Liquid Chromatography Mass Spectrometry (LCMS). Quantitative analysis of POX from skin extract samples collected in the skin decontamination experiment was performed by LCMS spectrometry using a Waters Acquity UPLC system equipped with a Waters TQ detector mass spectrometer as reported from our labs.^{1, 2} Its chromatographic system had an ODS column (Acquity UPLC BEH C₁₈ 1.7 μm ; 2.1 × 100 mm, with an XBridge C₁₈ 2.5 μm guard column, Waters) at a column temperature of 40 °C with a flow rate of 0.45 mL min⁻¹. Column elution was performed in a gradient mode with two mobile phases: 95% A (0–0.25 min), 95–0% A (0.25–7.75 min), 0% A (7.75–8.5 min), 0–95% A (8.5–8.51 min) over a 10 min cycle. Mobile phase A = 0.1% formic acid in 98 : 2 water : methanol; mobile phase B = 0.1% formic acid in methanol.

POX was detected using a method of multiple reaction monitoring (MRM) parameters (positive ionization mode; source temperature at 150 °C; desolvation temperature at 400 °C; cone

voltage at 27 V; collision energy at 20 eV). POX was identified as the species at $t_r = 6.0$ min in the LC trace which produced a parent mass (m/z) of 276.036. Its calibration curve was generated in the range of 1.0–250 nM that afforded a linear correlation of peak AUC = $1698.0 \times [\text{POX}]$ ($R^2 = 0.99$).

3. Methods of Oxime Synthesis

2 (Scheme S1)



reagents and conditions: (i) Ethylenediamine, EtOH, room temp, 3 h, quantitative; (ii) Formaldehyde, EtOH, 30 min; then NaCNBH₃, 50 °C, 16 h, 65.9%

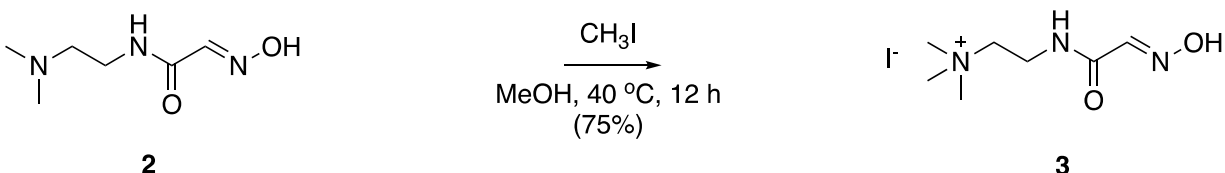
(2-(Hydroxyimino)-*N*-(2'-aminoethyl)acetamide) (**1**): To a flask containing a solution of ethylenediamine (255 mg, 4.26 mmol) in ethanol (2 mL) was added ethyl 2-(hydroxyimino)acetate¹ (166 mg, 1.42 mmol). The solution was magnetically stirred for 3 h under nitrogen gas atmosphere at room temperature and concentrated *in vacuo*. Volatile residues were fully removed by co-evaporation with ethanol (2 × 2 mL), and a resulting white solid was washed with cold ethanol (2 × 1 mL) and dried under higher vacuum. This led to a desired product (2-(hydroxyimino)-*N*-(2'-aminoethyl)acetamide) **1** as a solid (190 mg, quantitative). R_f (1:1 methanol/ethyl acetate) = 0.15. It was characterized by NMR and mass spectrometry, which was consistent with literature data.¹ HRMS (ESI) m/z : $[M + H]^+$: calcd for C₄H₁₀N₃O₂, 132.0773; found, 132.0765. ¹H NMR (500 MHz, CDCl₃): δ 8.06 (s, 1H, CH=NOH), 7.43 (s, 1H, CH=NOH), 5.58 (s, 1H, C(=O)NH), 3.12 (t, 2H, C(=O)NHCH₂), 2.59 (t, 2H, CH₂NH₂) ppm. ¹³C NMR (100 MHz, CDCl₃): δ 167.1, 143.3, 40.4, 39.6 ppm.

N-(2-(Dimethylamino)ethyl)-2-(hydroxyimino)acetamide (**2**): This oxime was prepared through reductive *N*-methylation of its precursor **1**. To **1** (65 mg, 0.50 mmol) was added excess formaldehyde in water (36.5–38%; 412 μ L, 5.6 mmol). The mixture was stirred at room temperature for 30 min prior to adding sodium cyanoborohydride (176 mg, 2.8 mmol) as a solid. The mixture was heated at 50 °C for 16 h, cooled to room temperature and treated with ethyl ether

(5 mL), which led to white precipitates. These were collected and washed with ether (2 × 5 mL). This crude product was further purified by a flash column chromatography by eluting with 10% methanol in dichloromethane, which afforded the desired product *N*-(2-(dimethylamino)ethyl)-2-(hydroxyimino)acetamide **2** as a white solid (52 mg, 65.9%). R_f (MeOH) = 0.1. Purity (UPLC): ≥95% (t_R = 1.98 min). MS (ESI) m/z (relative intensity, %) = 160.10 (100) [M + H]⁺. HRMS (ESI) calcd for C₆H₁₃N₃O₂ [M – H][–] 158.0930, found 158.0925. ¹H NMR (500 MHz, D₂O): δ 7.58 (s, 1H, CH=NOH), 3.59–3.57 (t, J = 5 Hz, 2H, CH₂NH), 2.99–3.01 (t, J = 5 Hz, 2H, CH₂N(CH₃)₂), 2.62 (s, 6H, 2CH₃) ppm. ¹³C NMR (500 MHz, D₂O): δ 165.3, 143.6, 56.5, 43.3, 35.3 ppm.

An alternative method for 2 (Scheme 1): To a flask containing a solution of *N*¹,*N*¹-dimethylethane-1,2-diamine (572 μL, 5.23 mmol) in ethanol (4 mL) was added ethyl 2-(hydroxyimino)acetate (204 mg, 1.74 mmol). The flask was stirred for 16 h under nitrogen gas atmosphere at room temperature and then heated at 45 °C for 2 h. The reaction mixture was concentrated *in vacuo*, and its residue was purified by flash column chromatography eluting with 10% methanol in dichloromethane. The desired product **2** was obtained as a white solid (72 mg, 26%) and its characterization data was fully consistent with those data acquired from **2** prepared from reductive *N*-methylation above.

3 (Scheme S2)



2-(2-(Hydroxyimino)acetamido)-*N,N,N*-trimethylethan-1-aminium iodide (**3**): This quaternary salt was prepared through *N*-methylation of **2** according to Gündisch, et al.³ To a solution of **2** (36.5 mg, 0.23 mmol) in methanol (0.4 mL) was added methyl iodide (30 μL, 0.38 mmol). The mixture was stirred at 40 °C overnight and then cooled to room temperature. The solid which precipitated was collected and washed with cold methanol (2 × 0.5 mL), affording 2-(2-(hydroxyimino)acetamido)-*N,N,N*-trimethylethan-1-aminium iodide **3** as a white solid (52 mg, 75.3%). R_f (MeOH) = 0.3. Purity (UPLC): ≥95% (t_R = 1.95 min). MS (ESI) m/z (relative intensity, %) = 174.1 (20) [M]⁺. HRMS (ESI) calcd for C₇H₁₆N₃O₂ [M]⁺ 174.1243, found 174.1236. ¹H NMR

(500 MHz, D₂O): δ 7.62 (s, 1H, CH=NOH), 3.82–3.79 (t, $J = 6.5$ Hz, 2H, CH₂NH), 3.56–3.53 (t, $J = 6.5$ Hz, 2H, CH₂N(CH₃)₃), 3.19 (s, 9H, 3CH₃) ppm. ¹³C NMR (500 MHz, D₂O): δ 165.5, 143.5, 56.6, 43.5, 35.7 ppm.

4 (Scheme S3)



N-(2-(Diethylamino)ethyl)-2-(hydroxyimino)acetamide (**4**): To a flask containing a solution of *N,N*-diethylethylenediamine (410 mg, 3.53 mmol) in ethanol (1.3 mL) was added ethyl 2-(hydroxyimino)acetate (138 mg, 1.18 mmol). The mixture was stirred under nitrogen gas atmosphere at 45 °C for 2 h when no change was detectable in the mixture by thin layer chromatography (TLC) analysis. The reaction mixture was cooled down overnight, and a white material which precipitated was collected, crystallized in ethanol (2 mL) and washed with cold ethanol (3 × 1 mL). The solid was dried *in vacuo*, yielding *N*-(2-(diethylamino)ethyl)-2-(hydroxyimino)acetamide **4** as a white solid (166 mg, 75.3%). R_f (MeOH) = 0.35. Purity (UPLC): $\geq 95\%$ ($t_r = 3.85$ min). MS (ESI) m/z (relative intensity, %) = 188.13 (90) [M + H]⁺. HRMS (ESI) calcd for C₈H₁₇N₃O₃ [M – H][–] 186.1243, found 186.1253. ¹H NMR (500 MHz, D₂O): δ 7.53 (s, 1H, CH=NOH), 3.58–3.56 (t, $J = 5$ Hz, 2H, CH₂NH), 3.08–3.06 (t, $J = 5$ Hz, 2H, Et₂NCH₂), 3.01–2.97 (q, $J = 6.7$ Hz, 4H, 2NCH₂), 1.19–1.16 (t, $J = 7.5$ Hz, 6H, 2CH₃) ppm. ¹³C NMR (500 MHz, D₂O): δ 166.4, 143.2, 50.5, 47.2, 34.9, 8.8 ppm.

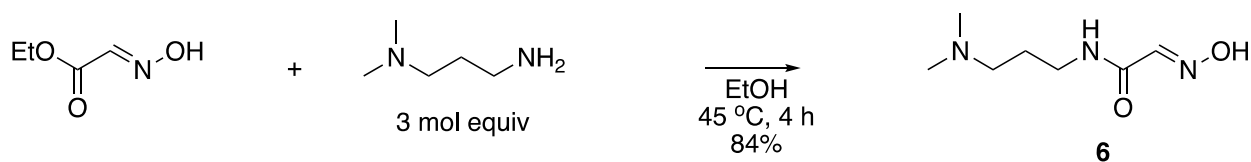
5 (Scheme S4)



2-(Hydroxyimino)-*N*-(2-(pyrrolidin-1-yl)ethyl)acetamide (**5**): To a flask containing a solution of 1-(2-aminoethyl)pyrrolidine (406 mg, 3.56 mmol) in ethanol (1.3 mL) was added ethyl 2-(hydroxyimino)acetate¹ (139 mg, 1.19 mmol). The solution was stirred for 4 h under nitrogen gas

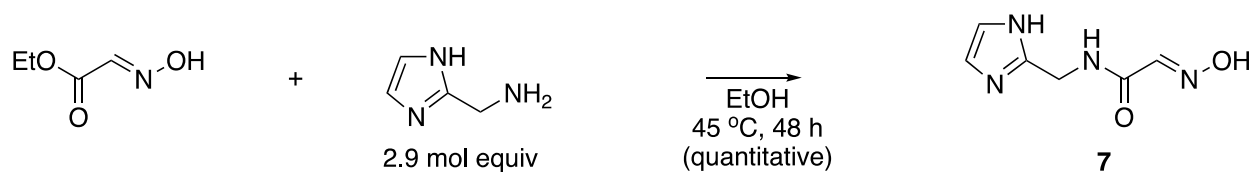
atmosphere at 45 °C. The solution was concentrated *in vacuo* and co-evaporated with ethanol (2 × 2 mL). Its solid residue was crystallized in ethanol and dried *in vacuo*, yielding 2-(hydroxyimino)-*N*-(2-(pyrrolidin-1-yl)ethyl)acetamide **5** as a white solid (173 mg, 78.7%). R_f (MeOH) = 0.25. Purity (UPLC): $\geq 95\%$ (t_r = 3.06 min). MS (ESI) m/z (relative intensity, %) = 186.12 (100) [M + H]⁺. HRMS (ESI) calcd for C₈H₁₅N₃O₂ [M – H][–] 184.1086, found 184.1107. ¹H NMR (500 MHz, D₂O): δ 7.54 (s, 1H, CH=NOH), 3.59–3.57 (t, J = 5 Hz, 2H, CH₂NH), 3.13–3.11 (t, J = 5 Hz, 2H, CH₂N), 3.08 (s, 4H, 2CH₂), 1.95 (s, 4H, 2CH₂) ppm. ¹³C NMR (500 MHz, D₂O): δ 166.3, 143.3, 53.9, 53.8, 36.3, 22.5 ppm.

6 (Scheme S5)



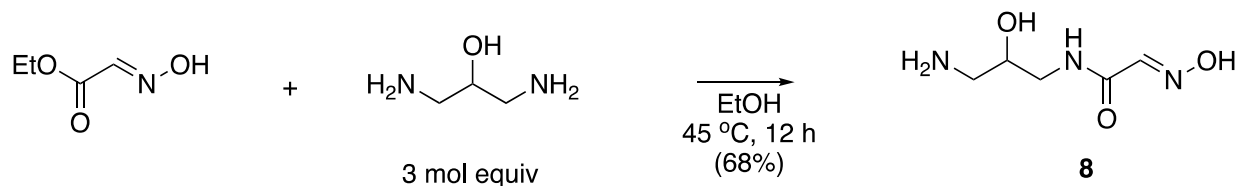
N-(3-(Dimethylamino)propyl)-2-(hydroxyimino)acetamide (**6**): To a flask containing a solution of 3-(dimethylamino)-1-propylamine (387 mg, 3.79 mmol) in ethanol (1.3 mL) was added ethyl 2-(hydroxyimino)acetate¹ (148 mg, 1.26 mmol). The flask was stirred under nitrogen gas atmosphere at 45 °C for 4 h or until no change was detected in the reaction mixture as monitored by TLC. The solution was concentrated *in vacuo* and volatile were fully removed by co-evaporation with 1-butanol (2 × 2 mL). The solid residue was crystallized in ethyl acetate and dried *in vacuo*, affording *N*-(3-(dimethylamino)propyl)-2-(hydroxyimino)acetamide **6** as a white solid (183 mg, 83.6%). R_f (MeOH) = 0.13. Purity (UPLC): $\geq 95\%$ (t_r = 2.26 min). MS (ESI) m/z (relative intensity, %) = 174.12 (90) [M + H]⁺. HRMS (ESI) calcd for C₇H₁₅N₃O₂ [M – H][–] 172.1086, found 172.1083. ¹H NMR (500 MHz, D₂O): δ 7.54 (s, 1H, CH=NOH), 3.36–3.33 (t, J = 6.5 Hz, 2H, CH₂NH), 3.86–3.89 (t, J = 6.5 Hz, 2H, CH₂N), 2.62 (s, 6H, 2CH₃), 1.92–1.86 (m, 2H, CH₂) ppm. ¹³C NMR (500 MHz, D₂O): δ 166.0, 143.3, 55.4, 43.0, 36.3, 24.8 ppm

7 (Scheme S6)



N-((1*H*-Imidazol-2-yl)methyl)-2-(hydroxyimino)acetamide (**7**): First, 2-(aminomethyl)imidazole, which was purchased as a dihydrochloride salt, was converted to a neutral amine. Its salt (428 mg, 2.52 mmol) was suspended in ethanol (4 mL) and treated with 2 molar equiv of sodium hydroxide (201 mg, 5.04 mmol) as solid. The mixture was stirred for 10 min and filtered off to remove a white solid formed (NaCl), which was followed by washing of the solid with ethanol (2 × 0.4 mL). Its filtrate and washing solutions were combined, and the amine solution was mixed with ethyl 2-(hydroxyimino)acetate¹ (103 mg, 0.88 mmol). The mixture was stirred under nitrogen gas atmosphere at 45 °C for 48 h. The solution was concentrated *in vacuo*, and its residue was washed with ethyl acetate (3 × 1 mL). The residue was further purified by flash column chromatography by eluting with 10–20 % methanol in dichloromethane, which led to the isolation of *N*-((1*H*-imidazol-2-yl)methyl)-2-(hydroxyimino)acetamide **7** as a white solid (194 mg, quantitative). *R_f* (MeOH) = 0.70. Purity (UPLC): ≥95% (*t_r* = 2.12 min). MS (ESI) *m/z* (relative intensity, %) = 169.07 (100) [M + H]⁺. HRMS (ESI) calcd for C₆H₈N₄O₂ [M – H][–] 167.0569, found 167.0567. ¹H NMR (500 MHz, CD₃OD): δ 7.65 (s, 1H, CH=NOH), 7.05 (s, 2H, CH₂-Im), 4.56 (s, 2H, CH₂NH) ppm. ¹³C NMR (500 MHz, D₂O): δ 164.3, 144.4, 143.7, 122.0, 36.2 ppm.

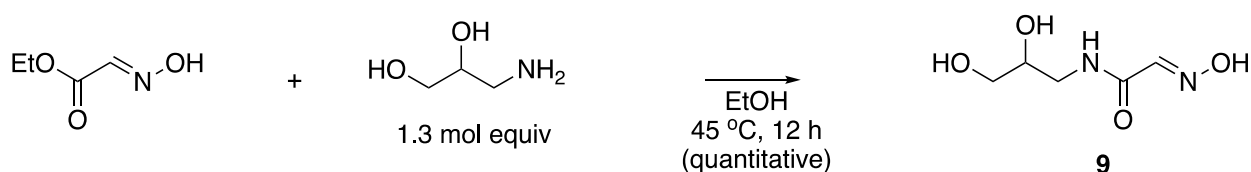
8 (Scheme S7)



N-(3-Amino-2-hydroxypropyl)-2-(hydroxyimino)acetamide (**8**): To a flask containing a solution of 1,3-diamino-2-propanol (408 mg, 4.53 mmol) in ethanol (4 mL) was added ethyl 2-(hydroxyimino)acetate¹ (177 mg, 1.5 mmol). The reaction mixture was stirred under nitrogen gas atmosphere at 45 °C for 12 h or until the reaction was completed as monitored by TLC. The mixture was concentrated *in vacuo*, yielding an oil residue. It was washed with ether (2 × 2 mL),

leading to precipitated white solid. It was crystallized in 1:1 ethyl acetate/ethanol yielding *N*-(3-amino-2-hydroxypropyl)-2-(hydroxyimino)acetamide **8** as a white solid (166 mg, 68.2%). R_f (MeOH) = 0.3. Purity (UPLC): $\geq 95\%$ (t_r = 1.72 min). MS (ESI) m/z (relative intensity, %) = 162.08 (100) $[M + H]^+$. HRMS (ESI) calcd for $C_5H_{11}N_3O_3$ $[M - H]^-$ 160.0722, found 160.0722. 1H NMR (500 MHz, D_2O): δ 7.59 (s, 1H, $\underline{CH=NOH}$), 3.96–3.93 (m, 1H, $\underline{CH-OH}$), 3.47–3.43 (dd, J_1 = 5 Hz, J_2 = 15 Hz, 1H, $1/2\underline{CH_2(NH)}$), 3.38–3.34 (dd, J_1 = 5 Hz, J_2 = 15 Hz, 1H, $1/2\underline{CH_2(NH)}$), 3.04–3.00 (dd, J_1 = 5 Hz, J_2 = 15 Hz, 1H, $1/2\underline{CH_2(NH_2)}$), 2.85–2.81 (dd, J_1 = 5 Hz, J_2 = 15 Hz, 1H, $1/2\underline{CH_2(NH_2)}$) ppm. ^{13}C NMR (500 MHz, D_2O): δ 165.6, 143.4, 67.7, 42.5, 42.3 ppm.

9 (Scheme S8)



N-(2,3-Dihydroxypropyl)-2-(hydroxyimino)acetamide (**9**): To a solution of 2-amino-1,3-propanediol (138 mg, 1.52 mol) in ethanol (2 mL) was added ethyl 2-(hydroxyimino)acetate¹ (161 mg, 1.14 mmol). The mixture was stirred under nitrogen gas atmosphere at 45 °C for 12 h or the reaction was completed by TLC analysis. The solution was concentrated *in vacuo*, and its resulting residue was washed with cold ethanol (2 × 0.2 mL). The solid was dried *in vacuo*, affording *N*-(2,3-dihydroxypropyl)-2-(hydroxyimino)acetamide **9** as a white solid (252 mg, quantitative). R_f (MeOH) = 0.5. Purity (UPLC): $\geq 95\%$ (t_r = 1.83 min). MS (ESI) m/z (relative intensity, %) = 162.08 (100) $[M]^+$. HRMS (ESI) calcd for $C_5H_{10}N_2O_4$ $[M - H]^-$ 161.0562, found 161.0559. 1H NMR (500 MHz, D_2O): δ 7.59 (s, 1H, $CH=N$), 3.96–3.93 (m, 1H, \underline{CHOH}), 3.47–3.43 (dd, J_1 = 5 Hz, J_2 = 10 Hz, 1H, $1/2\underline{CH_2OH}$), 3.38–3.34 (dd, J_1 = 5 Hz, J_2 = 10 Hz, 1H, $1/2\underline{CH_2OH}$), 3.04–3.00 (dd, J_1 = 5 Hz, J_2 = 10 Hz, 1H, $1/2\underline{CH_2NH}$), 2.85–2.81 (dd, J_1 = 5 Hz, J_2 = 10 Hz, 1H, $1/2\underline{CH_2NH}$) ppm. ^{13}C NMR (500 MHz, D_2O): δ 164.4, 143.9, 70.0, 63.1, 41.6 ppm.

4. Parallel Artificial Membrane Permeability Assay (PAMPA)

The permeability assay was performed using a PAMPA kit (PION, Inc.) according to its manufacturer's protocol. In a typical setting, each test solution (0.2 mM) was prepared in PBS pH 7.4 and loaded in donor plate wells (volume = V_D = 0.15 mL) which were pre-treated with a

solution of lecithin in dodecane (1% w/v) to generate a synthetic membrane of phospholipids. The loaded donor plate was then placed into the acceptor plate with its wells pre-loaded with PBS pH 7.4 (volume = $V_A = 0.3$ mL). After incubation for 4 or 6 h at room temperature (23 ± 2 °C), well solutions were carefully collected from the donor and acceptor plate and their oxime concentrations were determined through UV–vis analysis relative to reference spectra.

Permeability rate (P_e , cm s^{-1}) was calculated using Eq 1 and Eq 2 with parameters as defined in literature:^{4, 5}

$$P_e = -2.303 \times V_A \times V_D / [(V_A + V_D) \times A \times t] \times \log[1 - (V_A + V_D)C_{A(t)} / (V_D \times S \times C_{D(t=0)})] \quad \text{Eq 1}$$

$$S = (V_A \times C_{A(t)} + V_D \times C_{D(t)}) / (V_D \times C_{D(t=0)}) \quad \text{Eq 2}$$

where $C_{D(t)}$ and $C_{A(t)}$ refer to the concentration of the test solution collected from the donor and acceptor well at time t , respectively, $C_{D(t=0)}$ is the concentration of each test solution (0.2 mM) prior to permeation, A refers to the filter area (0.2826 cm^2) of the donor well, and t refers to permeation time (s).

5. AChE Assay

Two types of AChE were used that include *Electrophorus electricus* AChE (eAChE) and human recombinant AChE (hAChE), both from Sigma-Aldrich. Their assay was performed according to the Ellman's protocol⁶ using acetylthiocholine (ATCh) as its substrate in PBS pH 8.0 at ambient temperature (23 °C).⁶⁻⁸ The enzyme kinetics was monitored spectrophotometrically by reading absorbance (A) at 412 nm. For high-throughput readings, the assay was run using 96-well microplates placed in a plate reader (BioTek, Synergy) as described in our earlier works.^{1, 2} The first order rate constant k_{active} for a fully active enzyme was obtained by plotting $A_{412 \text{ nm}}$ against time (min) and calculating its slope ($\Delta A_{412 \text{ nm}} / \Delta t$; min^{-1}) at an early linear phase (0–15 min).

IC₅₀ (half-maximal inhibitory concentration) of OP. Experiments for AChE inactivation by OP were performed by treating AChE (0.2 U/mL) with OP (POX, CPS, MAL, OME) within a range of concentrations (10^{-9} – 10^{-6} M). After 30 min incubation, its residual activity was measured according to the assay protocol. The rate constant k_{OP} for AChE treated with OP at a given concentration was obtained and used to calculate its relative activity (%) as defined in Eq 3:

$$\text{Enzyme activity (\%)} = 100 \times (k_{\text{OP}} - k_{\text{inactive}})/(k_{\text{active}} - k_{\text{inactive}}) \quad \text{Eq 3}$$

where k_{active} and k_{inactive} each refers to the rate constant determined for AChE alone (fully active) or AChE + OP added maximally (fully inactivated), respectively. IC₅₀ values for each OP in eAChE and hAChE were estimated from its dose-enzyme activity (%) curves through a linear or non-linear regression analysis.

Oxime effect on enzyme activity. Experiments were performed in a similar manner as above but otherwise by replacing OP with selected oxime compounds at higher concentrations (10^{-6} – 10^{-3} M). Their rate constant (k_{oxime}) was determined and used to calculate relative enzyme activity as defined in Eq 3 by replacing k_{OP} with k_{oxime} .

Enzyme reactivation. AChE (0.2 U/mL) was inhibited to less than 5% of its original activity by treatment with OP at a concentration greater than IC₅₀ (Table S1): [POX] = 50 nM (hAChE), 500 nM (eAChE); [CPS] = 50 nM (hAChE, eAChE); [MAL] = 250 nM (eAChE). It was then treated with a series of oxime compounds including 2-PAM in a variable range of concentrations (10^{-5} – 10^{-3} M). After 30 min, the oxime-treated enzyme solutions were assayed to determine their rate constant ($k_{\text{OP} + \text{oxime}}$) in enzyme activity according to the protocol described above. The efficiency of enzyme reactivation is reported as % activity as shown in Eq 4:⁹

$$\text{Reactivation activity (\%)} = 100 \times [(k_{\text{OP} + \text{oxime}} - k_{\text{inactive}})/(k_{\text{active}} - k_{\text{inactive}})] \quad \text{Eq 4}$$

6. Spectrometric Screening of Chemical Reactivity in POX Inactivation

Reaction kinetics for POX inactivation by oxime was performed by spectrometric analysis as reported previously.^{1, 2, 10} Its reaction progress was monitored by focusing on time-dependent growth in absorbance by its byproduct 4-NP at 400 nm (λ_{max}). This spectrometric assay was performed using 96-well microplates in a plate reader (BioTek, Synergy). In a representative procedure, an oxime solution (8.0 mM) formulated in PBS at pH 8.0 or 10.5 was loaded in a 96-well microplate in triplicate (n = 3) and serially diluted to prepare a range of test concentrations (1.0–8.0 mM at pH 8.0 or 0.5–4.0 mM at pH 10.5, each 0.18 mL per well). The reaction kinetics was initiated by adding a POX solution (0.30 mM, 0.02 mL) freshly prepared in the same pH media to each oxime-containing well. Immediately, the microplate was read for its initial absorbance values at 400 nm in a plate reader. The plate was then continuously kept at ambient

temperature (17 ± 2 °C) or in an incubator controlled at 37 ± 1 °C over 3 days while it was temporarily removed for periodic readings at variable time points as specified in Figures S7–S9.

Data were processed and analyzed for rate constant determination as described in earlier works.¹⁰ Each absorbance (A_t) read at time t was processed to calculate the amount of 4-NP produced using its calibration curve ($[4\text{-NP}]_t = (1.01 \times 10^{-4} \text{ M}) \times A_t$), and its amount was used to calculate the amount of intact POX at time t indirectly by its subtraction from the initial POX amount ($[\text{POX}]_t = 3.0 \times 10^{-5} \text{ M} - [4\text{-NP}]_t$).

Calculation of Rate Constants. As defined in Figure 4, kinetic rate parameters (k_{obsd} , k_1) of POX inactivation were extracted according to a second-order rate law (Eq 5) and under a pseudo-first order condition (Eq 6) in which the oxime concentration is assumed to remain almost unchanged due to its catalytic nature and a large molar excess relative to POX.

$$\text{Rate} = -d[\text{POX}]/dt = k_1[\text{POX}][\text{Oxime}] \quad \text{Eq 5}$$

$$\text{Rate} = k_{\text{obsd}}[\text{POX}] \text{ where } k_1[\text{Oxime}] \approx k_{\text{obsd}} \quad \text{Eq 6}$$

$$\ln[\text{POX}]_t = \ln[\text{POX}]_{t=0} - k_{\text{obsd}}t \quad \text{Eq 7}$$

The observed rate constant k_{obsd} of an oxime compound varies linearly against test concentration (Eq 7), and it was determined as the slope through regression analysis ($R^2 \geq 0.95$). Each k_{obsd} value is reported as an average derived from at least three independent runs ($n \geq 3$). It was used to determine bimolecular rate constant k_1 according to Eq 6 by plotting k_{obsd} values against oxime concentrations and acquiring the slope (k_1 , $\text{M}^{-1} \text{ min}^{-1}$) as illustrated in Figure 4B.

7. Skin Decontamination *In Vitro*

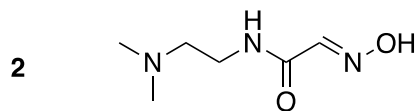
Topical decontamination of POX by oxime was performed as described in our earlier works.^{1, 2, 10} Porcine skin which was dehaired and 1.5 mm thick (Stellen Medical, LLC) was clamped as a test tissue between the donor and acceptor compartment in a Franz cell device controlled at 37 °C (Figure 7A). The donor side was loaded with a POX solution (50 μM , 0.4 mL) in 0.5% DMSO, PBS pH 10.5 and incubated for 2 min prior to loading a decontaminant solution of Dekon 139 or a test compound (0.3 M, 0.4 mL) formulated in PBS pH 10.5. The fully loaded device kept for 2

h while analyte solutions were periodically aliquoted from the donor side at multiple time points as specified in Figure 7. After the 2 h treatment, the skin tissue was recovered, processed and treated with 100% EtOH (1.0 mL) to extract POX penetrated. In addition, an analyte was aliquoted from the acceptor side at the end of the experiment ($t = 2\text{h}$).

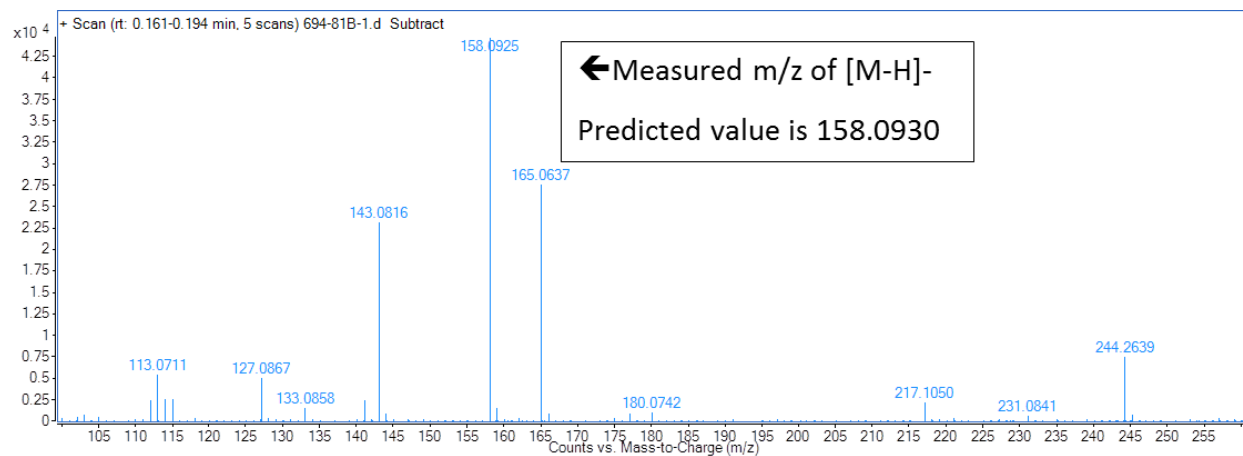
Analyte samples were analyzed for POX amounts by either UPLC or LC mass spectrometry (LCMS) as described in detail earlier.^{1, 2, 11} UPLC was used to analyze aliquot samples collected from the donor side. The concentration of POX at each time point was determined from the area under curve (AUC) analysis of the POX peak ($t_r = 10.3$ min) using its calibration curve. POX decay curves were constructed by plotting of intact POX (%) against decontamination time (Figure 5) and used to calculate POX half-life values from the regression analysis of their decay functions. POX half-life values are presented each as a mean acquired from two detection wavelengths at 215 and 275 nm.

LC mass spectrometry (MS/MS) was employed to analyze samples from skin extracts and the acceptor compartment. It was performed in a Waters TQ detector mass spectrometer using a positive ionization mode and multiple reaction monitoring (MRM) parameters as described earlier.^{1, 2, 11} It was equipped with a Waters Acquity LC system for the chromatographic separation of analytes. POX was detected as a species at $t_r = 6.0$ min in the LC trace with a parent mass (m/z) of 276.036 in the mass analysis. The concentration of POX was calculated by AUC analysis of its ion counts using a calibration curve generated in the range of 1.0 nM to 250 nM: $\text{AUC} = 1698.0 \times [\text{POX}]$ ($R^2 = 0.99$). The rate of skin penetration is arbitrarily defined here as the amount of POX (ng) detected per tissue weight (g) per treatment time (h): (unit = $\text{POX ng} \times (\text{skin tissue g} \times \text{h})^{-1}$).

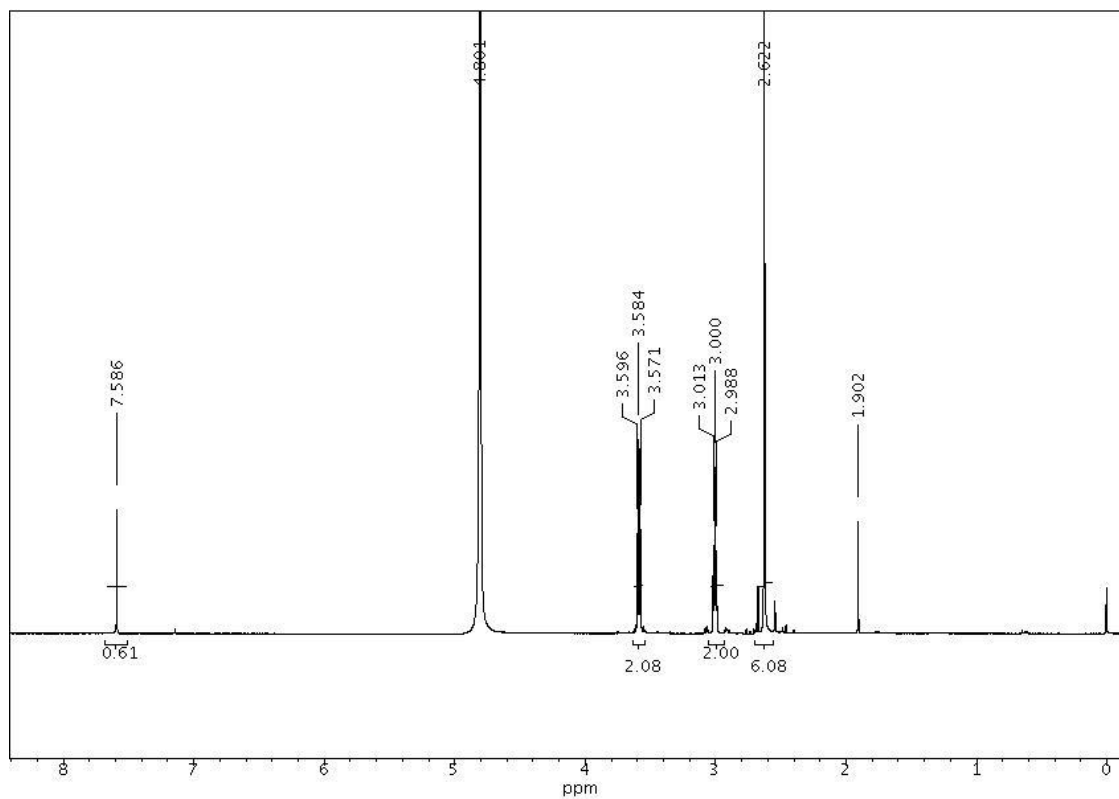
8. Copies of spectral data (high resolution mass spectra, ^1H & ^{13}C NMR spectra)



(A) Ion counts vs mass-to-charge (m/z): $[\text{M} - \text{H}]^-$ calcd for $\text{C}_6\text{H}_{13}\text{N}_3\text{O}_2^-$, 158.0930, found 158.0925



(B) ^1H NMR (D_2O , 500 MHz)



(C) ^{13}C NMR (D_2O , 100 MHz)

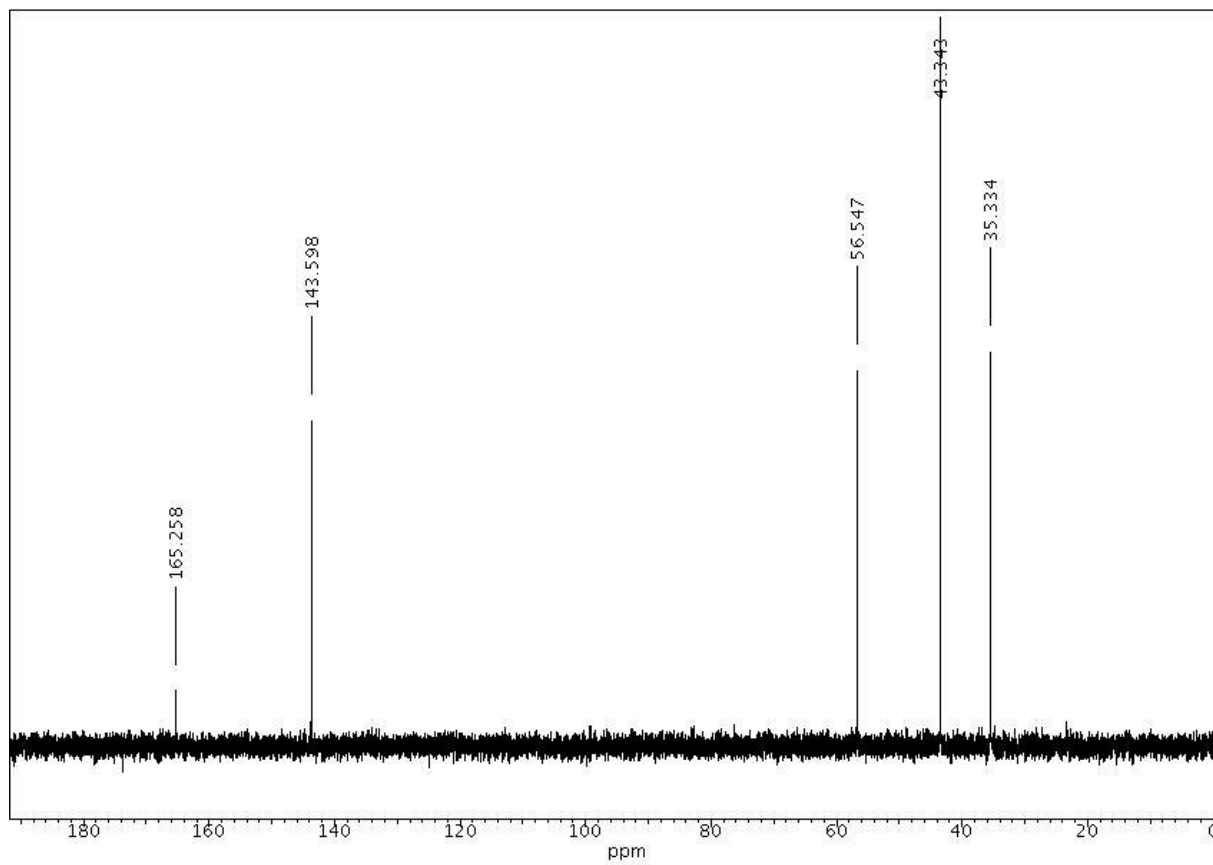
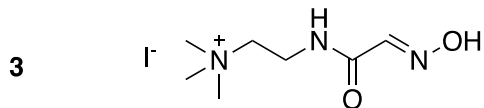
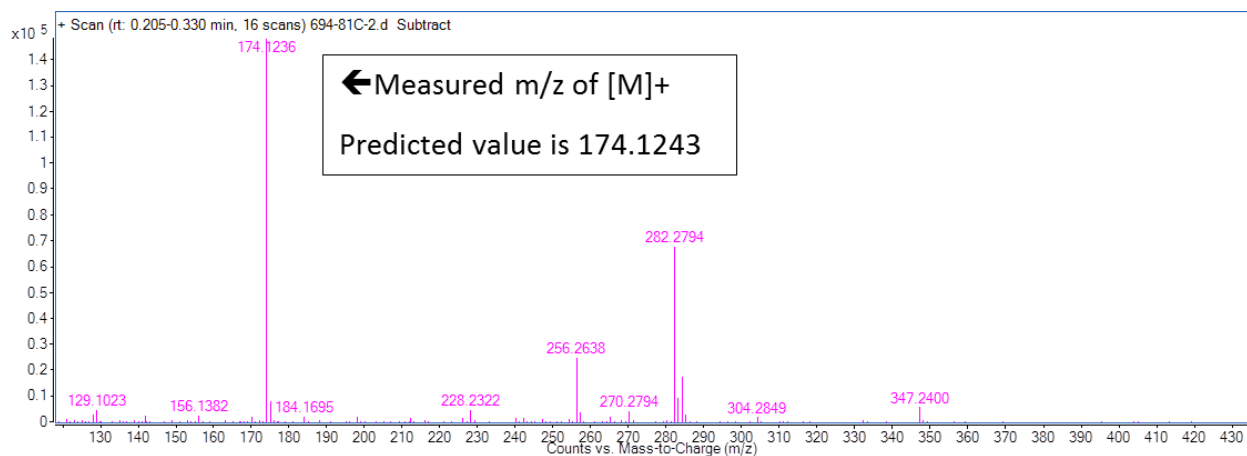


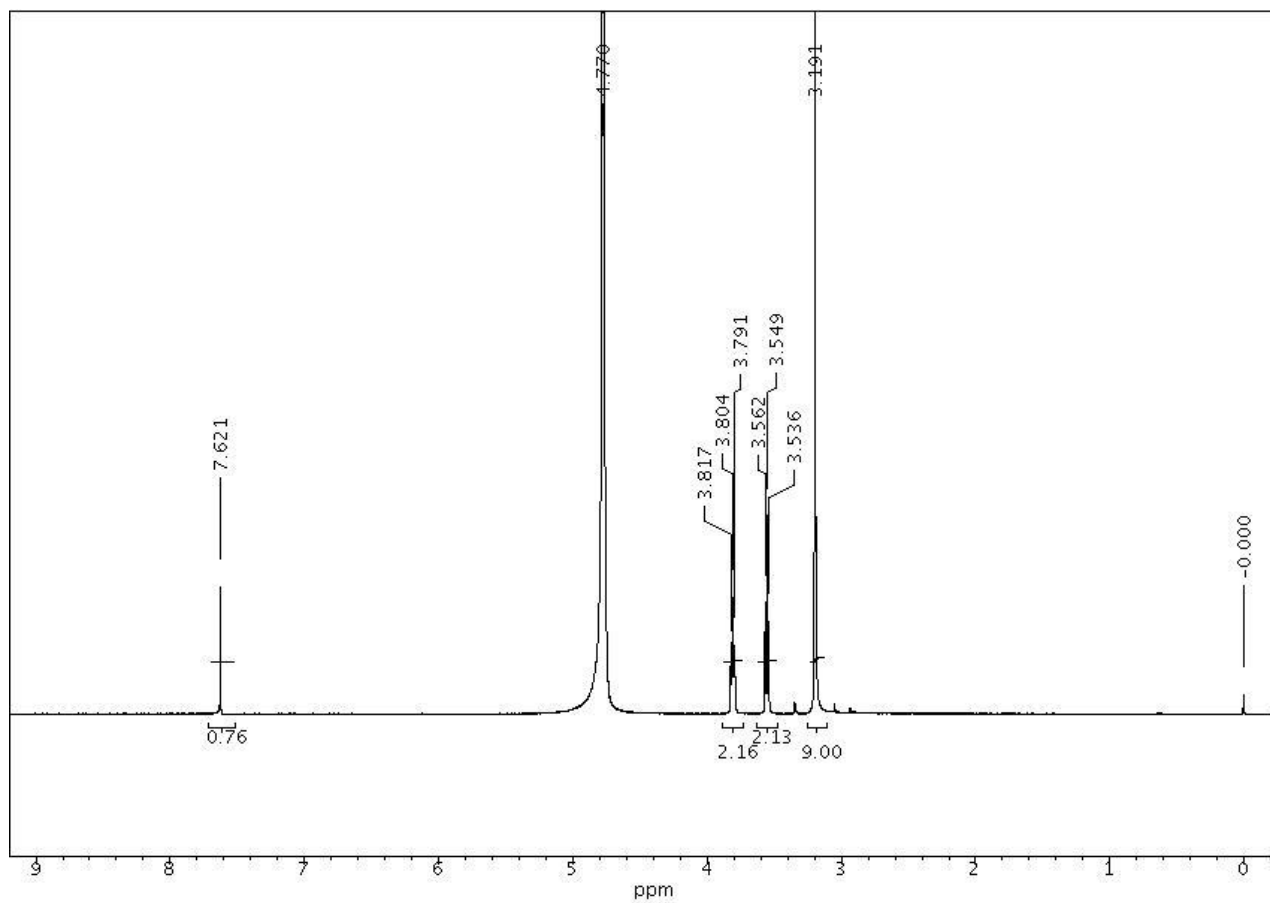
Figure S1-1. (A) High resolution mass spectrum, (B) ^1H NMR and (C) ^{13}C NMR spectra of **2**



(A) Ion counts vs mass-to-charge (m/z): $[M]^+$ calcd for $C_7H_{16}N_3O_2^+$, 174.1243, found 174.1236



(B) 1H NMR (D_2O , 500 MHz)



(C) ^{13}C NMR (D_2O , 100 MHz)

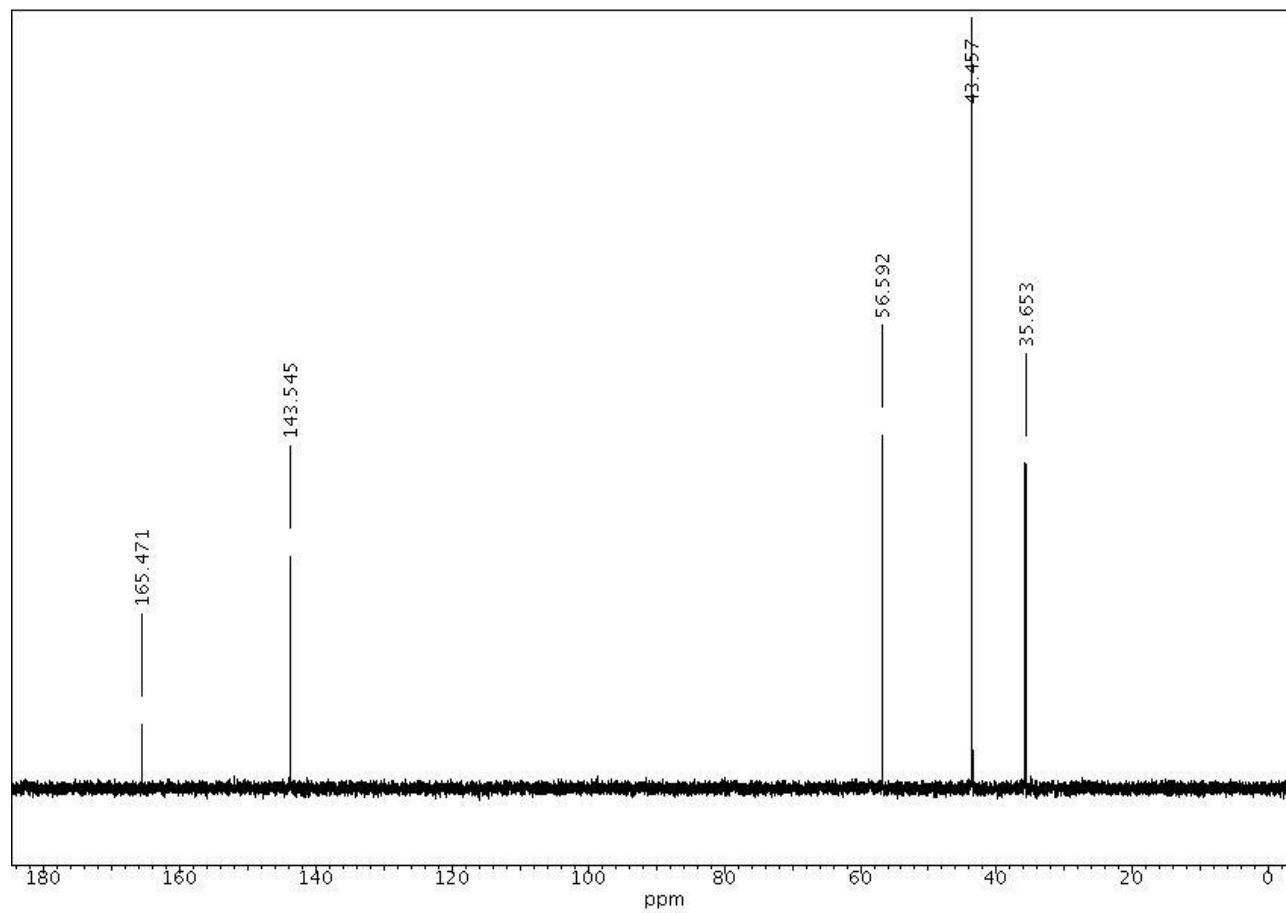
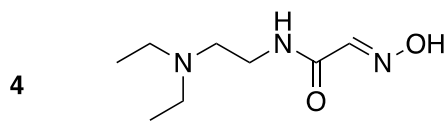
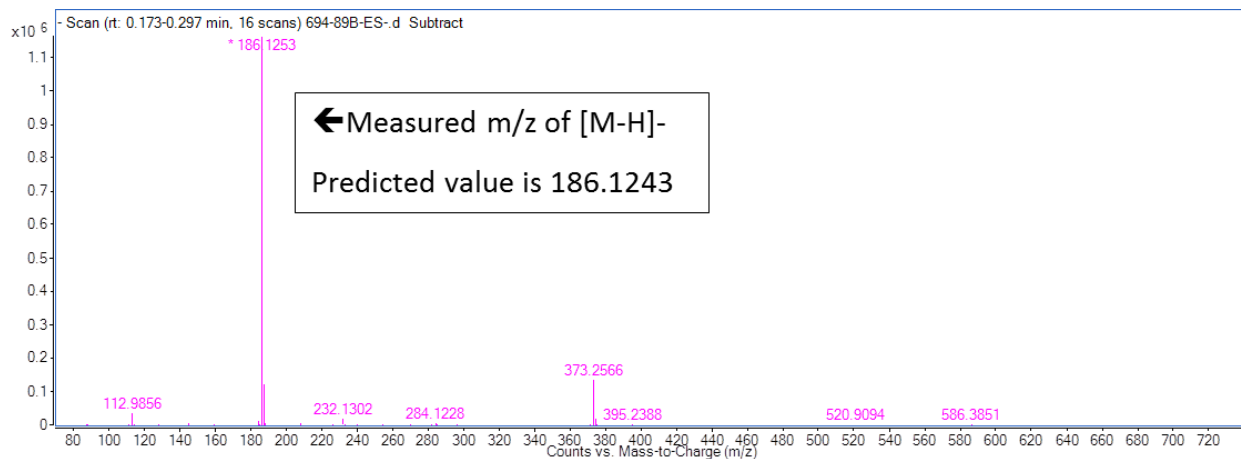


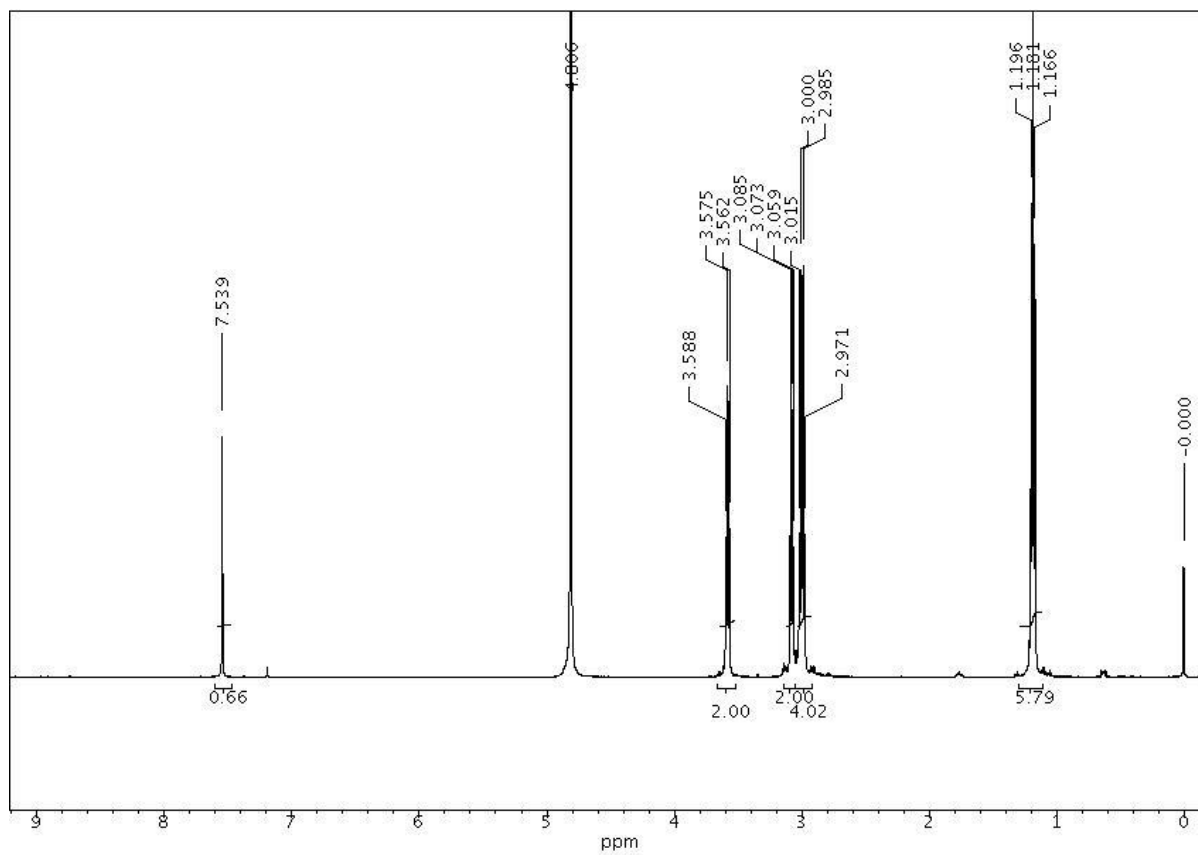
Figure S1-2. (A) High resolution mass spectrum, (B) ^1H NMR and (C) ^{13}C NMR spectra of **3**



(A) Ion counts vs mass-to-charge (m/z): $[M - H]^-$ calcd for $C_8H_{17}N_3O_3^-$, 186.1243, found 186.1253)



(B) 1H NMR (D_2O , 500 MHz)



(C) ^{13}C NMR (D_2O , 100 MHz)

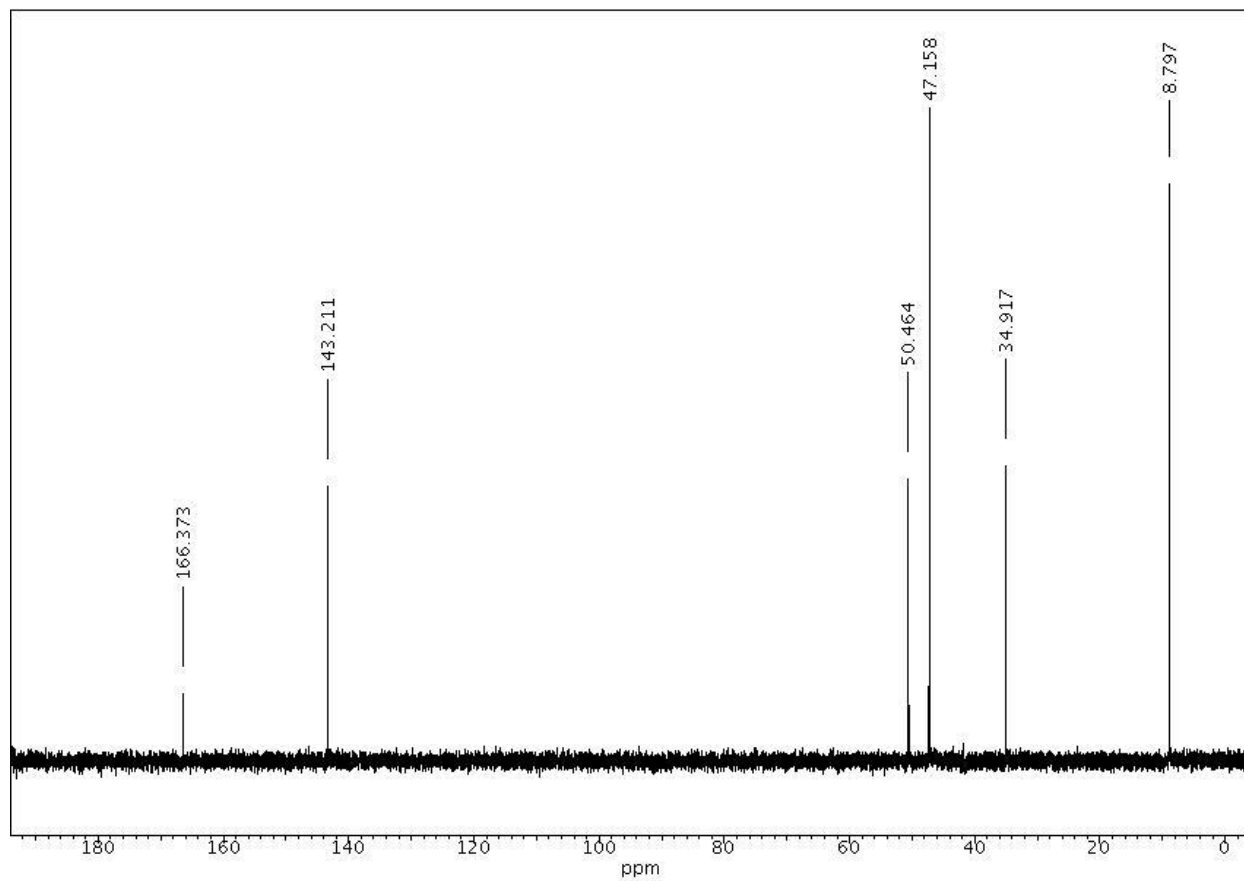
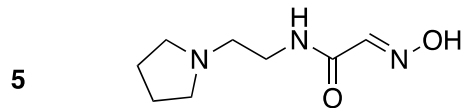
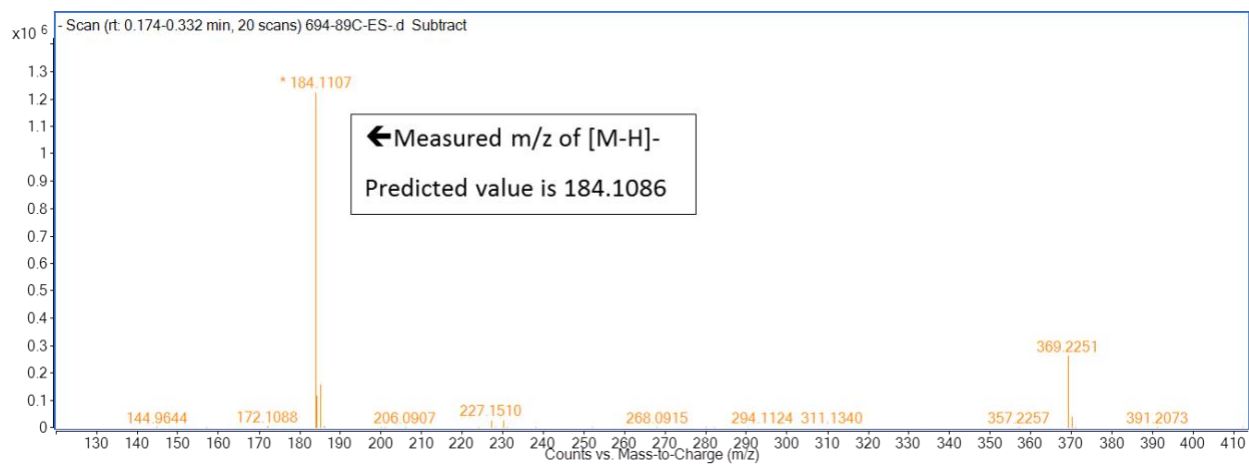


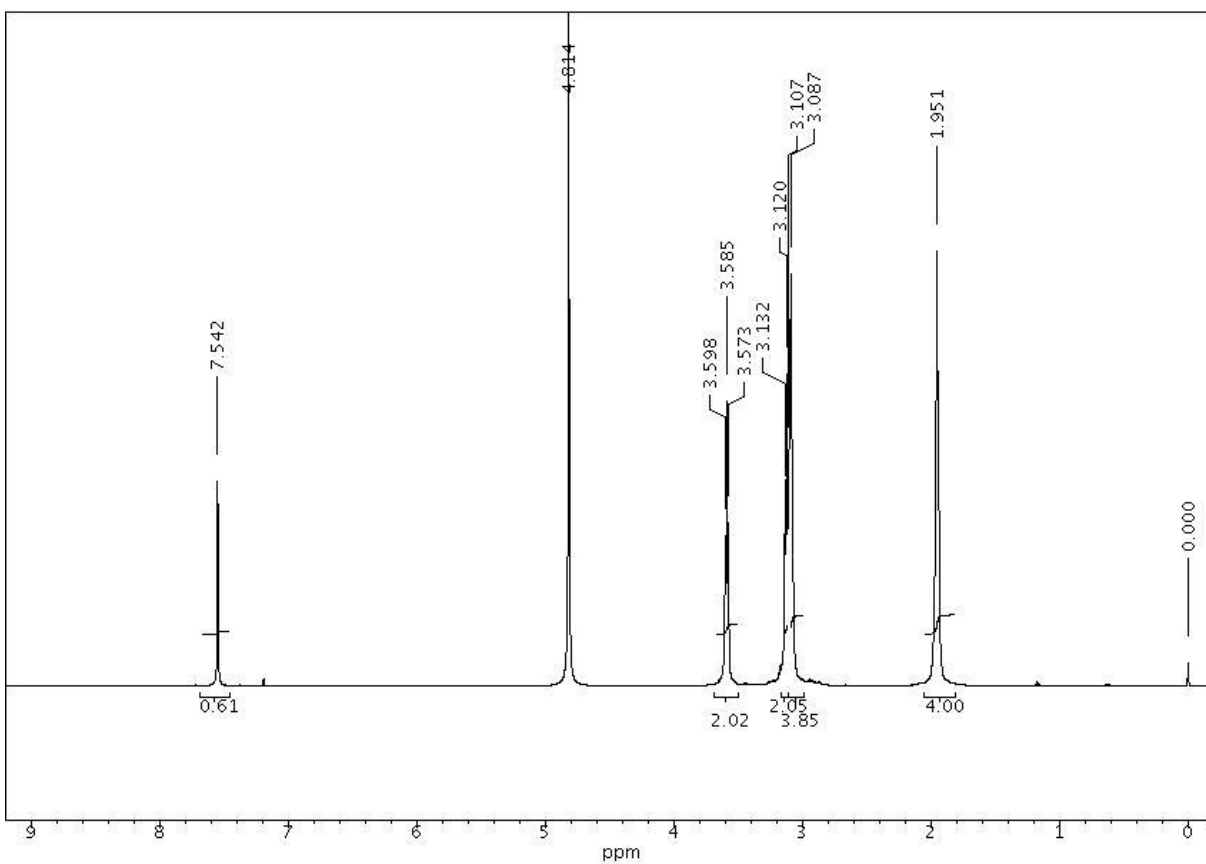
Figure S1-3. (A) High resolution mass spectrum, (B) ^1H NMR and (C) ^{13}C NMR spectra of **4**



(A) Ion counts vs mass-to-charge (m/z): $[M - H]^-$ calcd for $C_8H_{15}N_3O_2^-$, 184.1086, found 184.1107)



(B) 1H NMR (D_2O , 500 MHz)



(C) ^{13}C NMR (D_2O , 100 MHz)

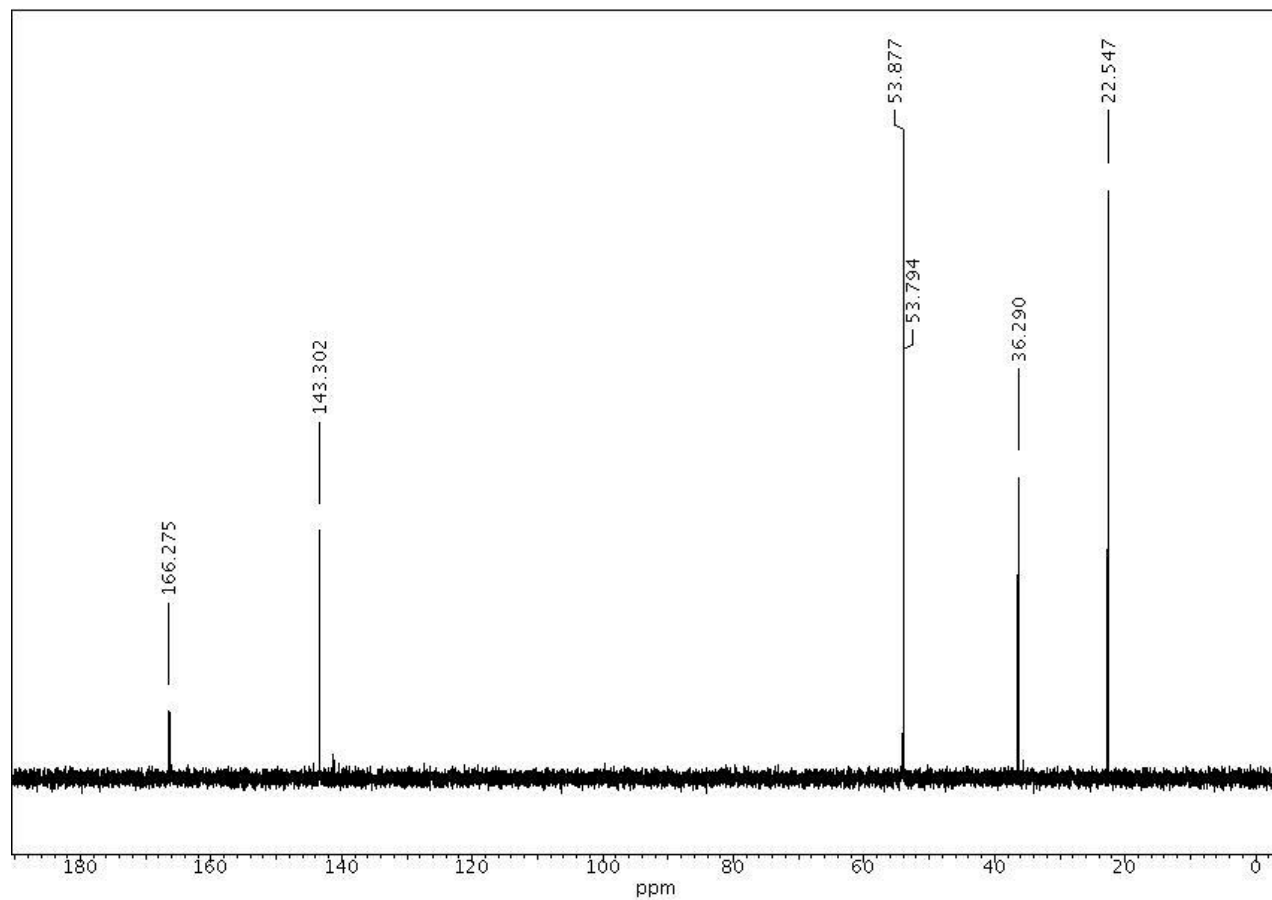
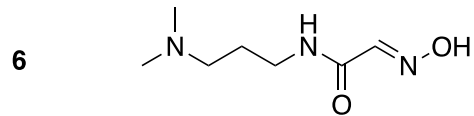
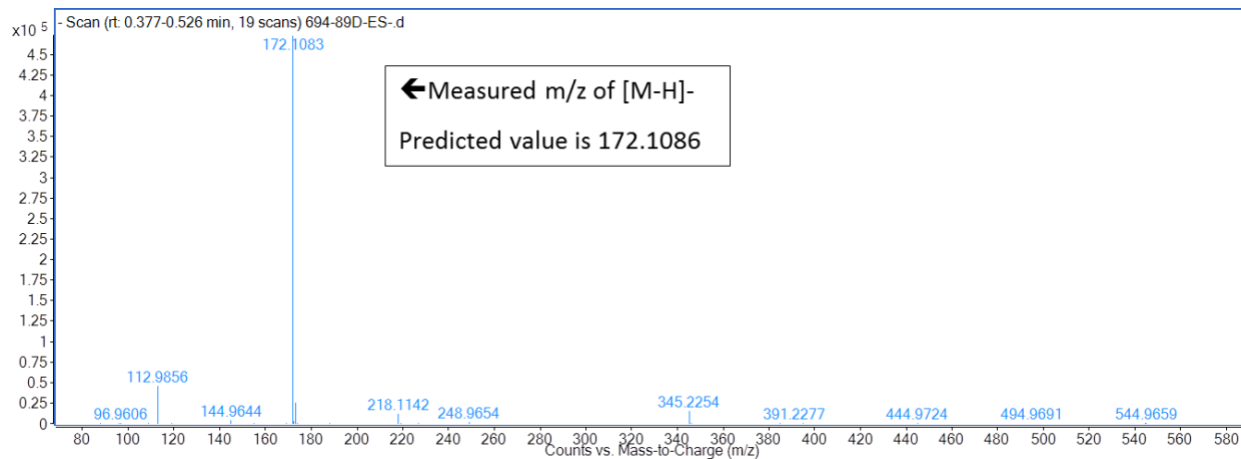


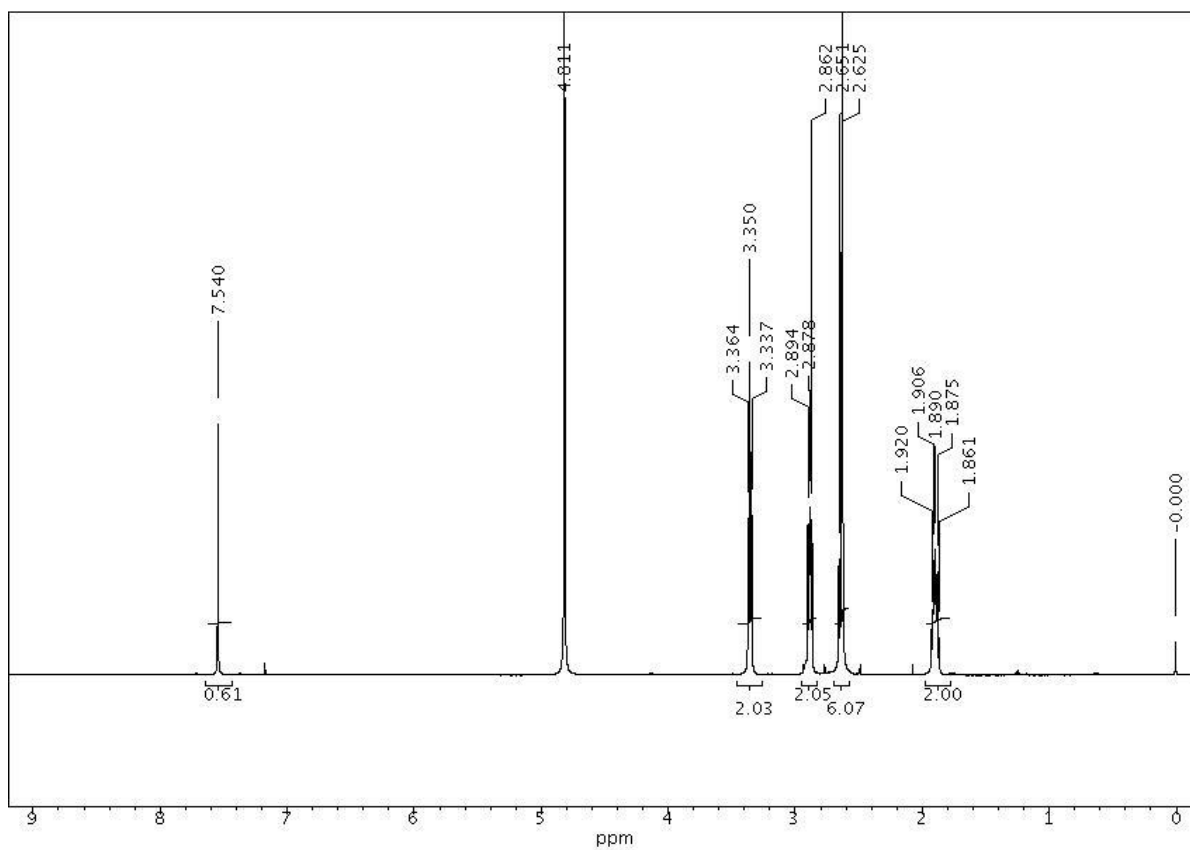
Figure S1-4. (A) High resolution mass spectrum, (B) ^1H NMR and (C) ^{13}C NMR spectra of **5**



(A) Ion counts vs mass-to-charge (m/z): $[M - H]^-$ calcd for $C_7H_{15}N_3O_2^-$, 172.1086, found 172.1083)



(B) 1H NMR (D_2O , 500 MHz)



(C) ^{13}C NMR (D_2O , 100 MHz)

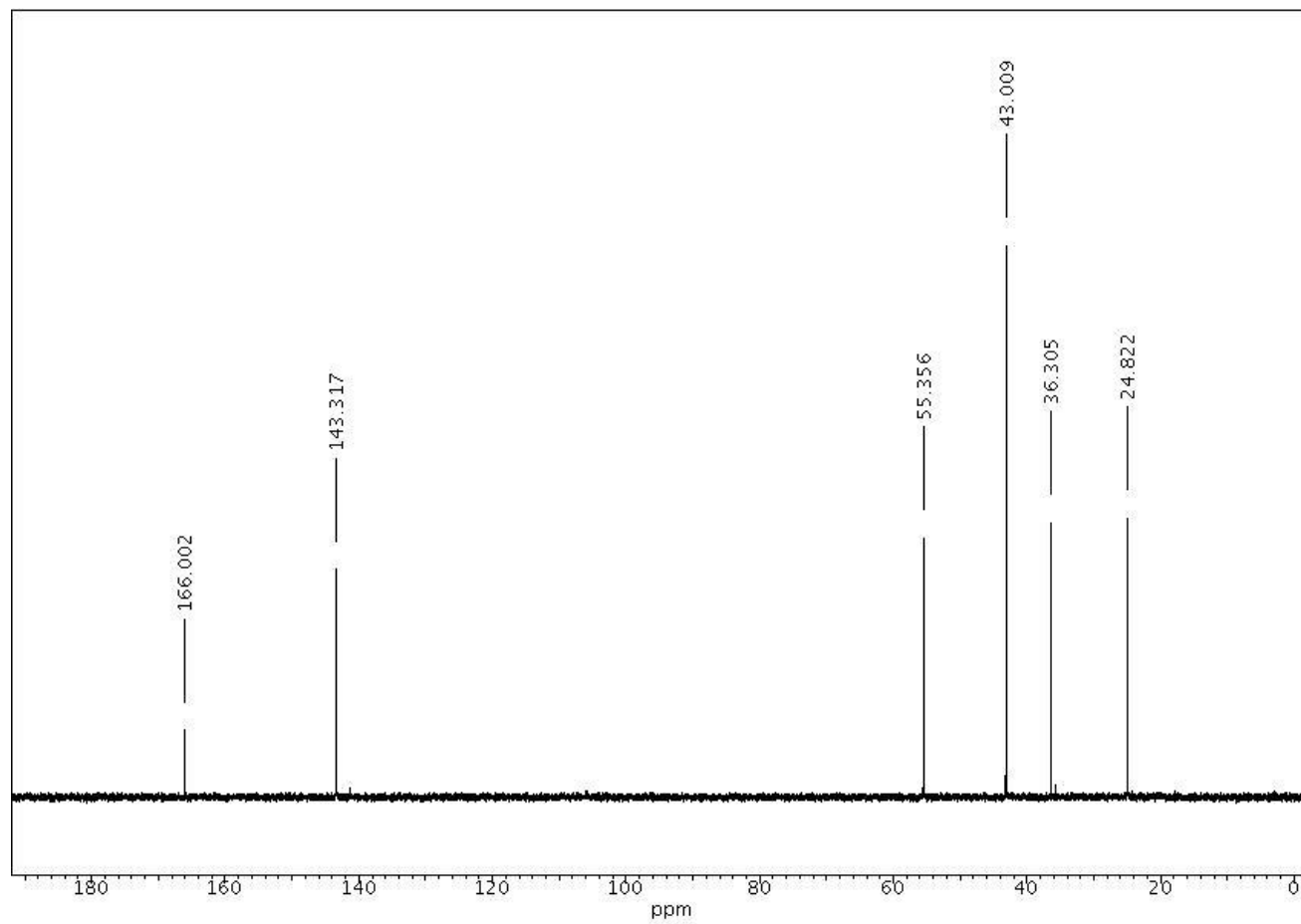
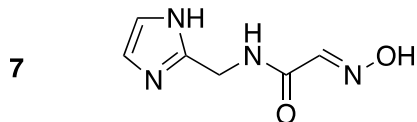
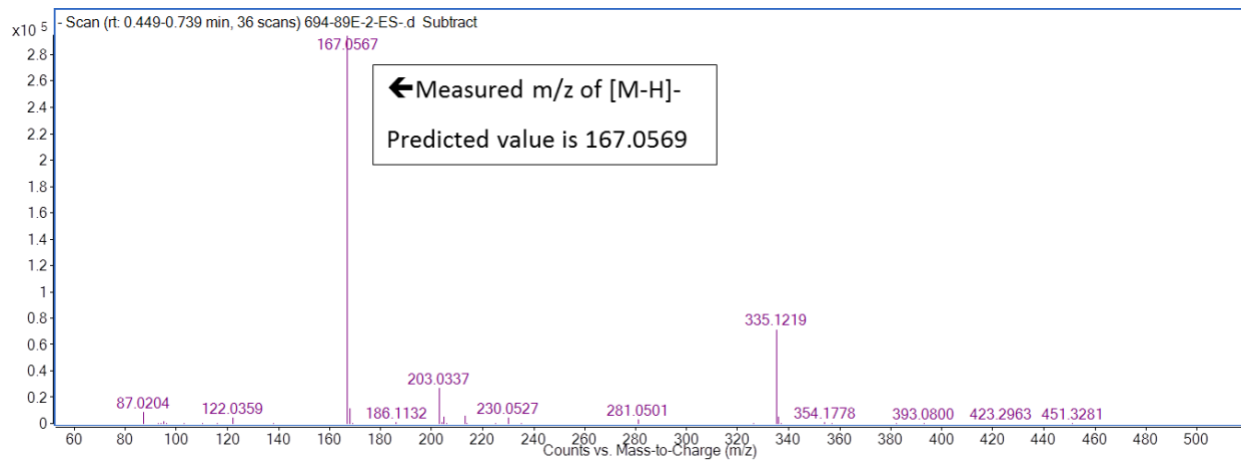


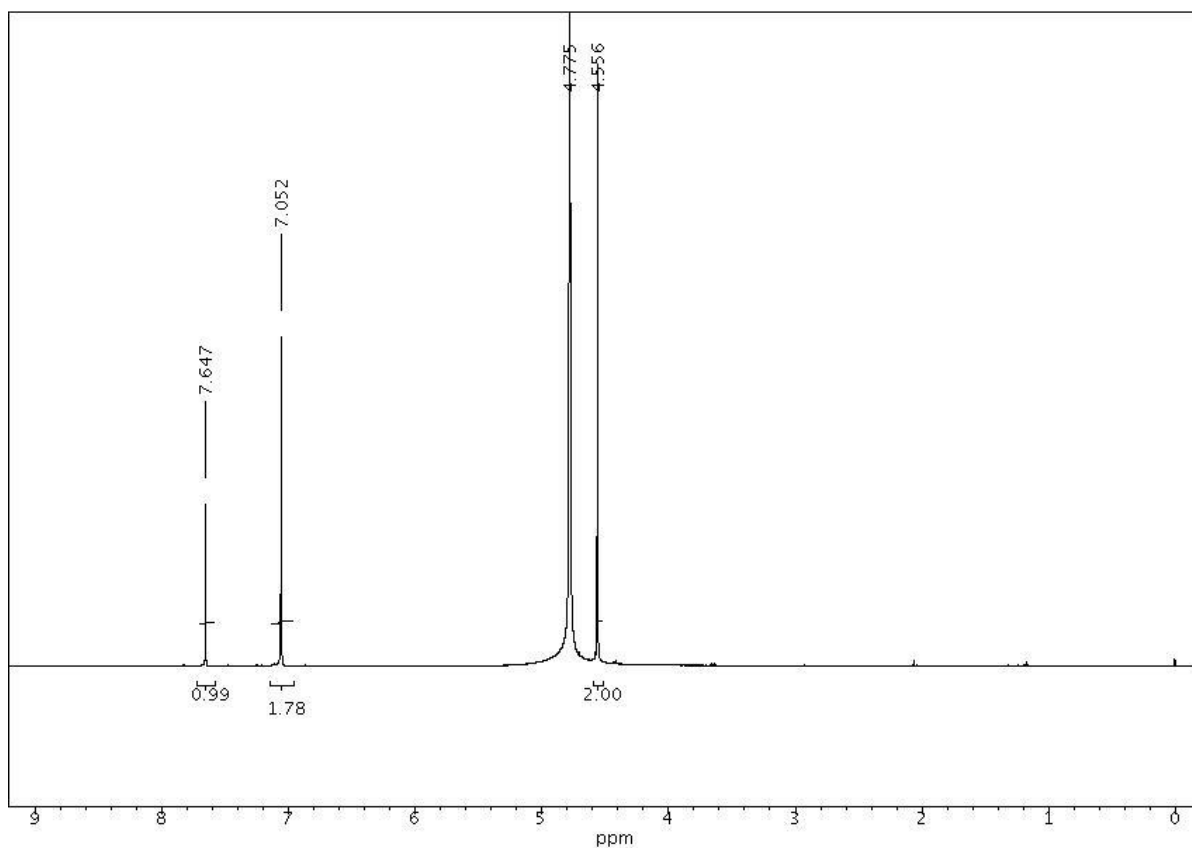
Figure S1-5. (A) High resolution mass spectrum, (B) ^1H NMR and (C) ^{13}C NMR spectra of **6**



(A) Ion counts vs mass-to-charge (m/z): $[M - H]^-$ calcd for $C_6H_8N_4O_2^-$, 167.0569, found 167.0567)



(B) 1H NMR (D_2O , 500 MHz)



(C) ^{13}C NMR (D_2O , 100 MHz)

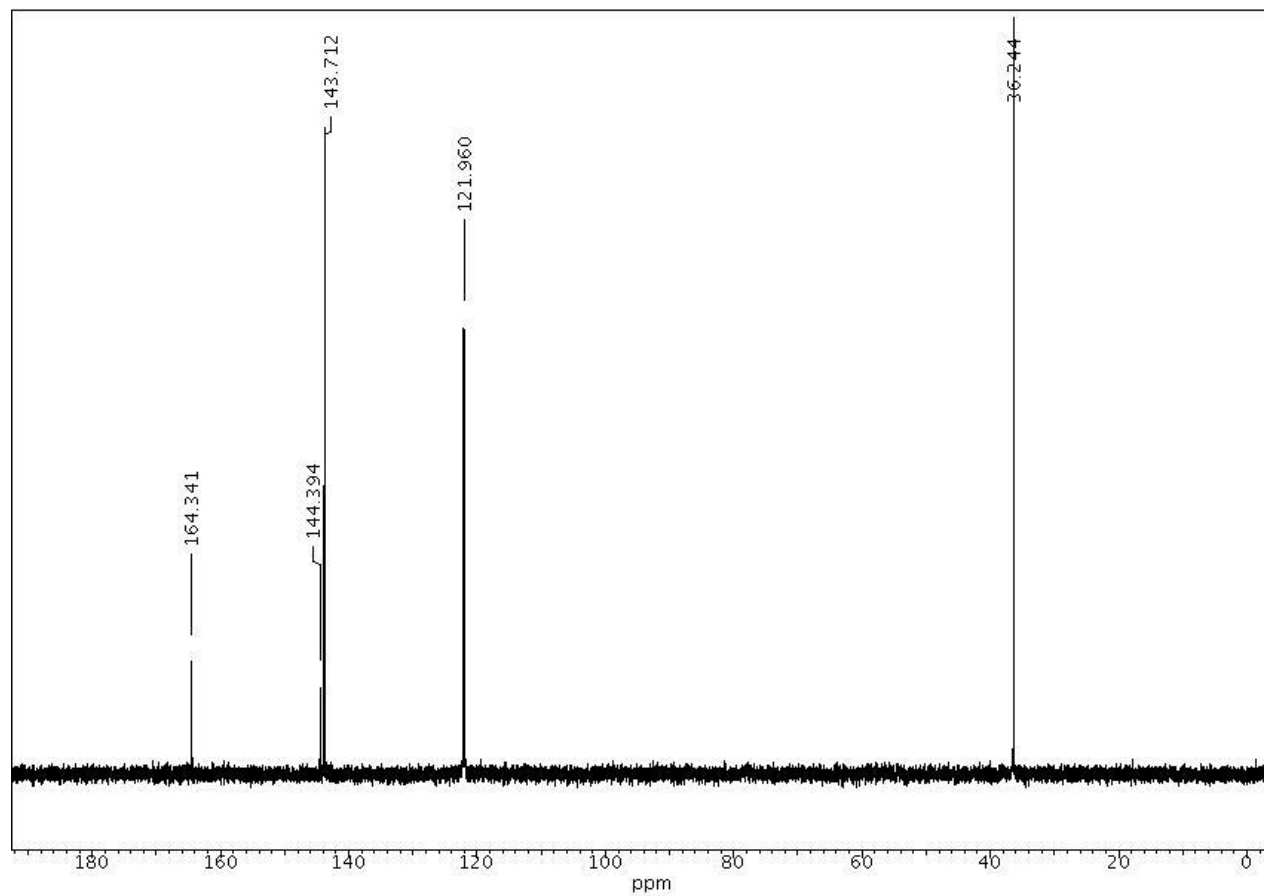
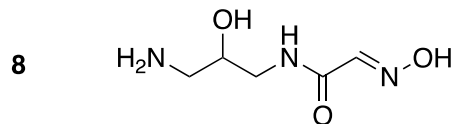
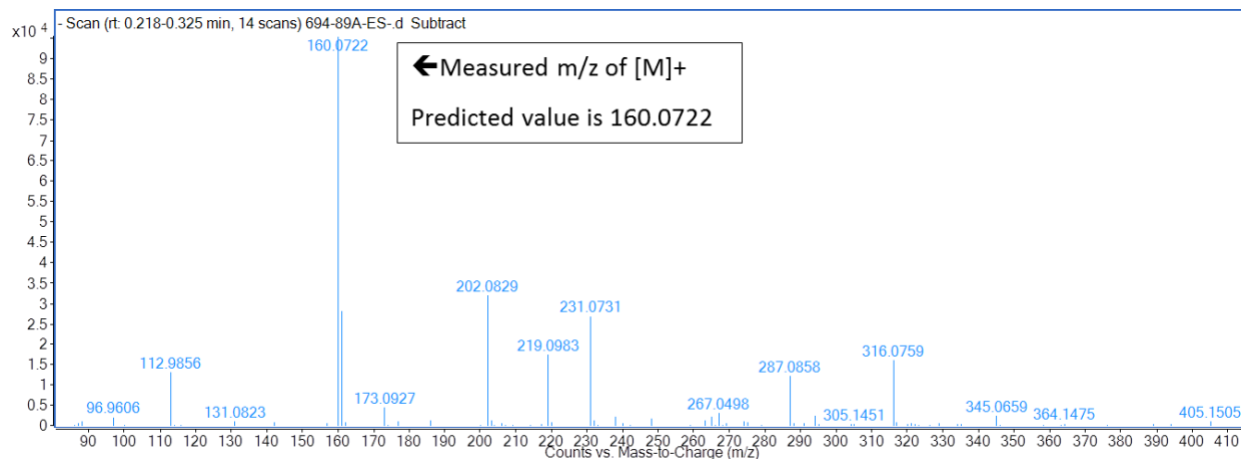


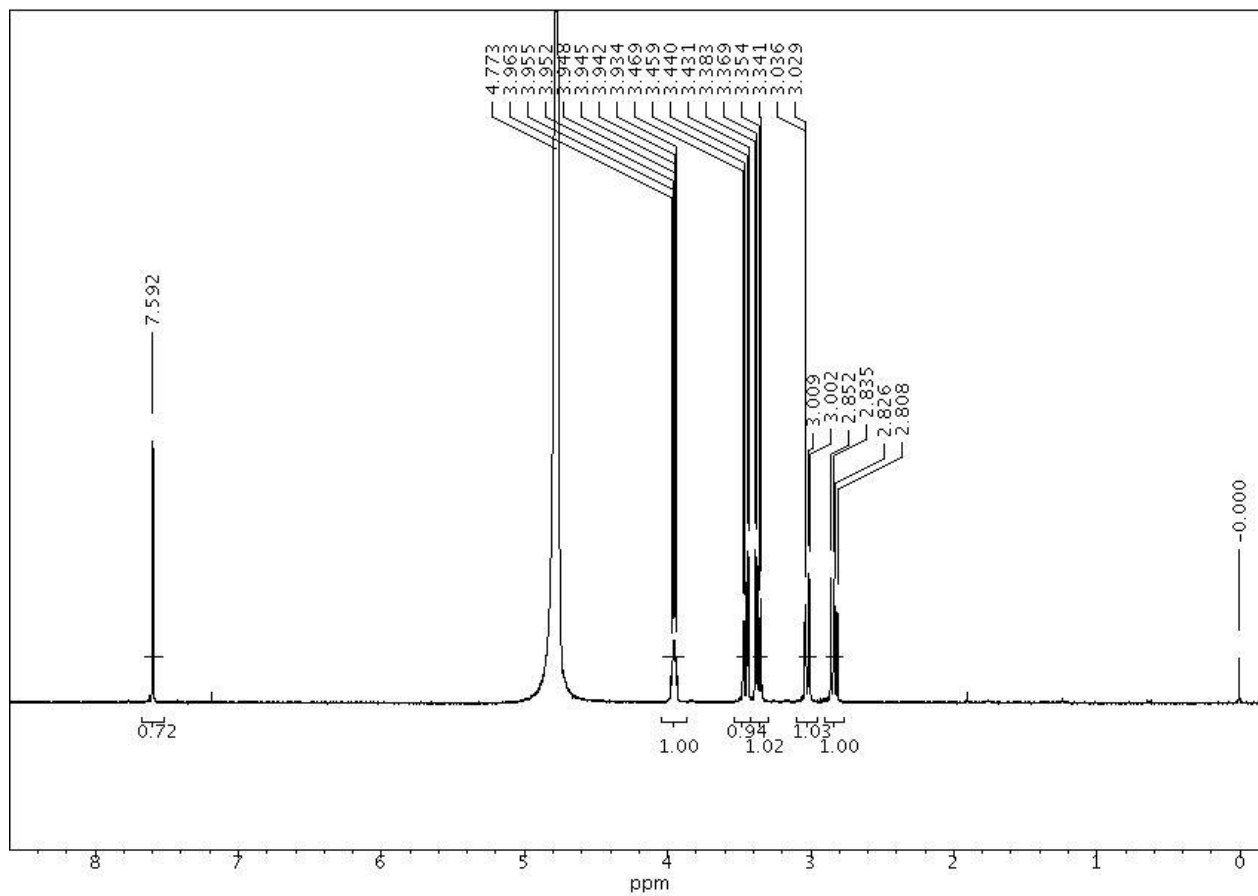
Figure S1-6. (A) High resolution mass spectrum, (B) ^1H NMR and (C) ^{13}C NMR spectra of **7**



(A) Ion counts vs mass-to-charge (m/z): $[M]^+$ calcd for $C_5H_{11}N_3O_3^+$, 160.0722, found 160.0722)



(B) 1H NMR (D_2O , 500 MHz)



(C) ^{13}C NMR (D_2O , 100 MHz)

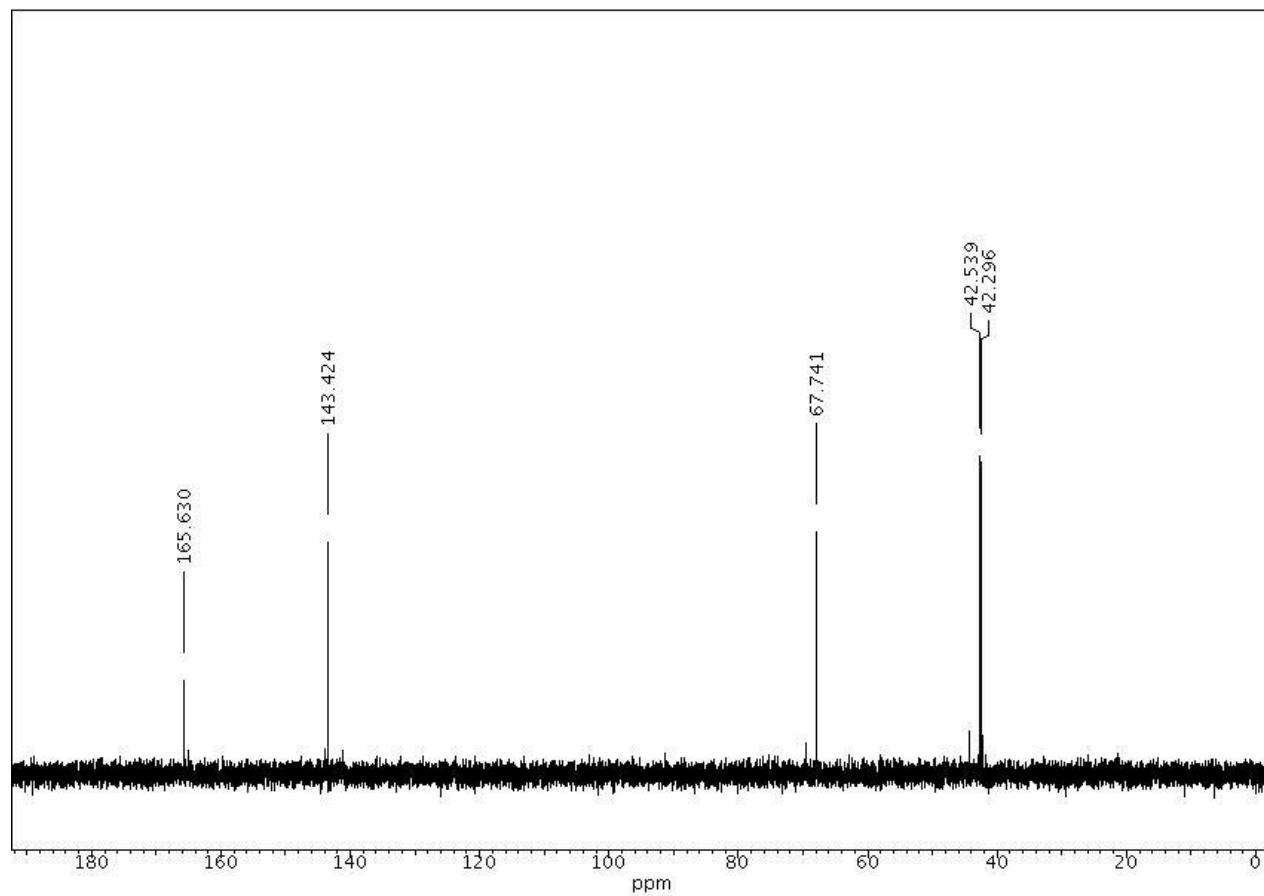
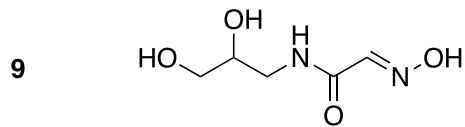
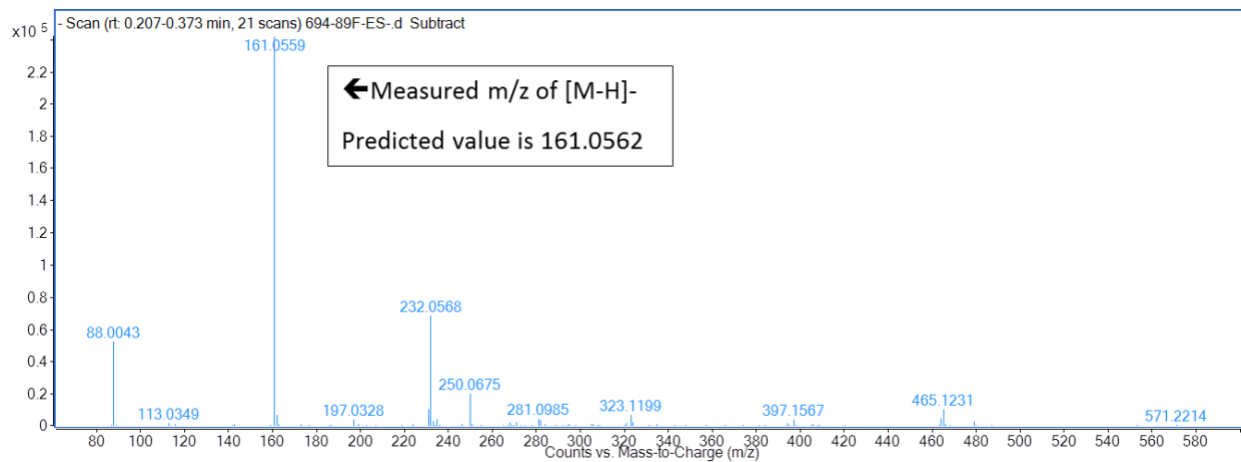


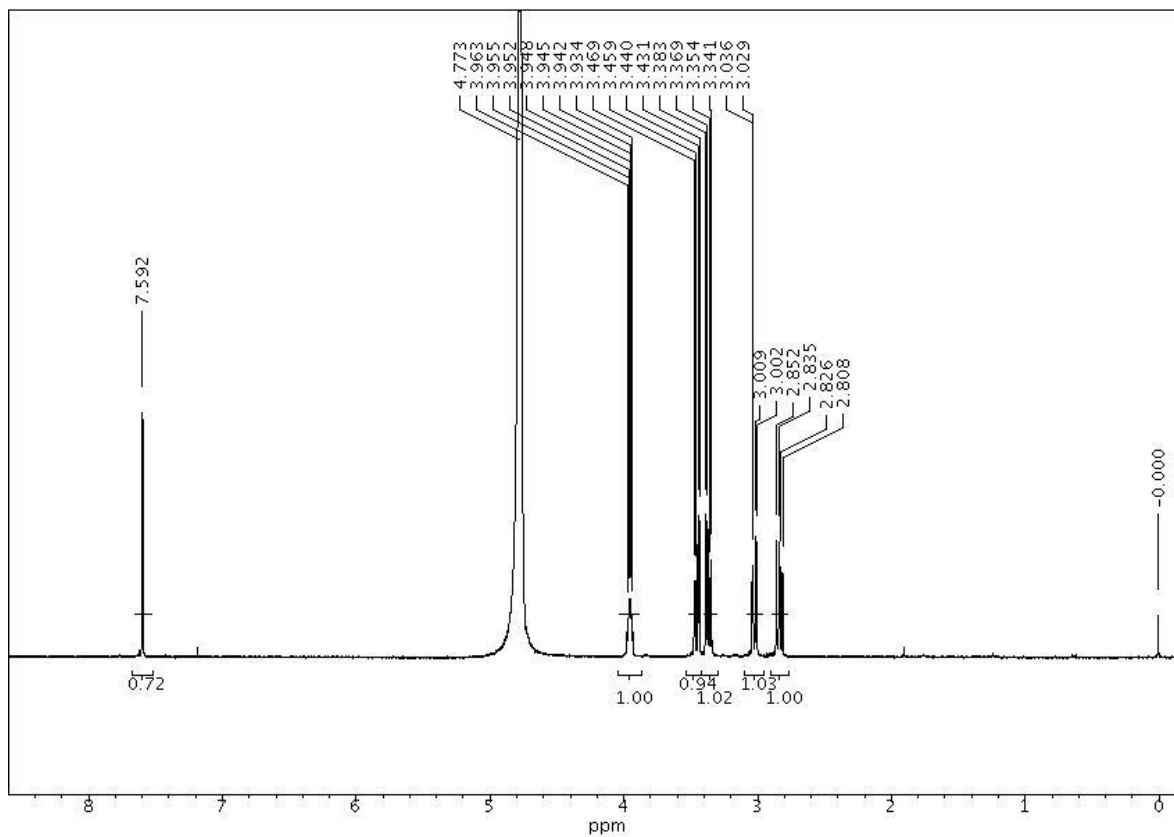
Figure S1-7. (A) High resolution mass spectrum, (B) ^1H NMR and (C) ^{13}C NMR spectra of **8**



(A) Ion counts vs mass-to-charge (m/z): $[M - H]^-$ calcd for $C_5H_{10}N_2O_4^-$, 161.0562, found 161.0559)



(B) 1H NMR (D_2O , 500 MHz)



(C) ^{13}C NMR (D_2O , 100 MHz)

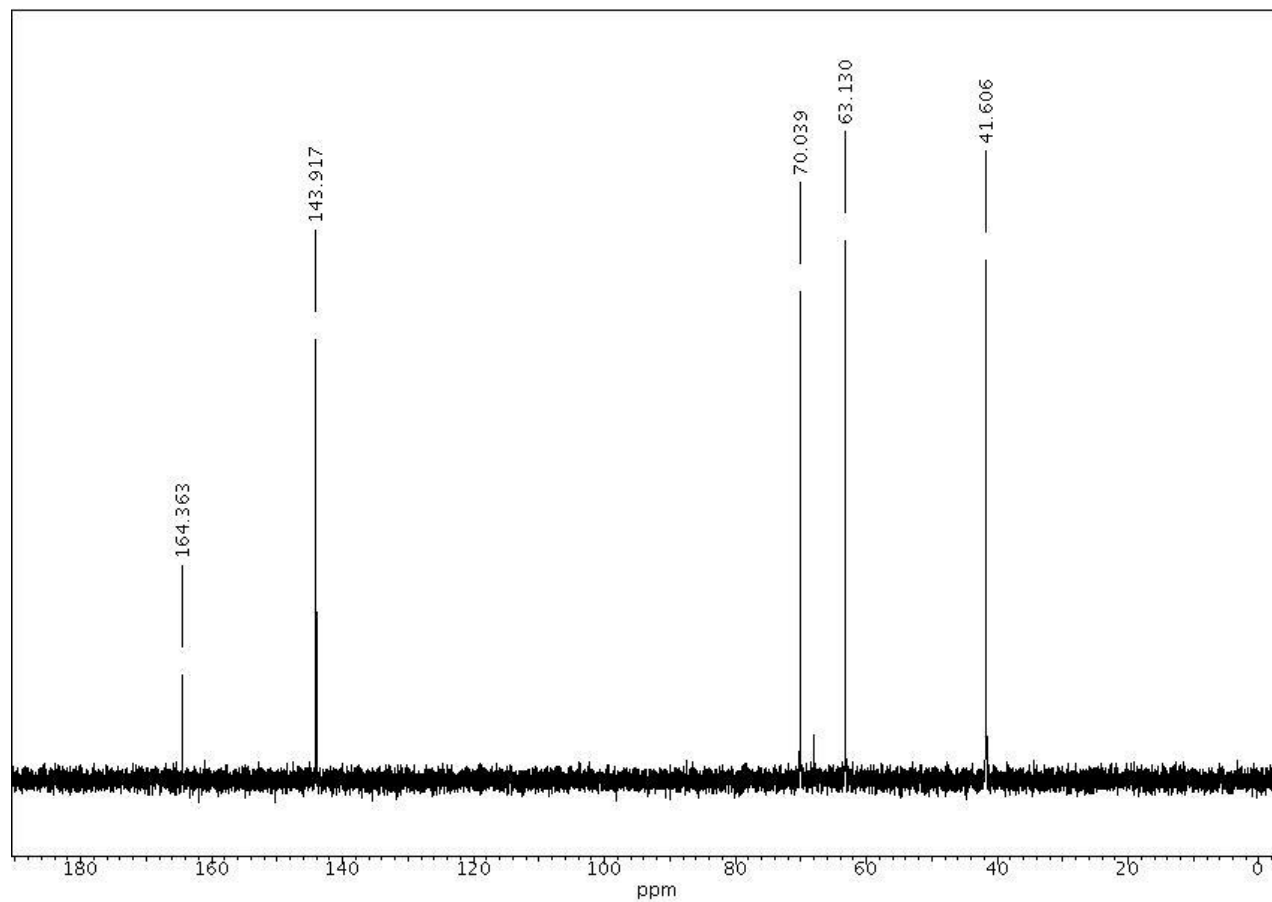


Figure S1-8. (A) High resolution mass spectrum, (B) ^1H NMR and (C) ^{13}C NMR spectra of **9**

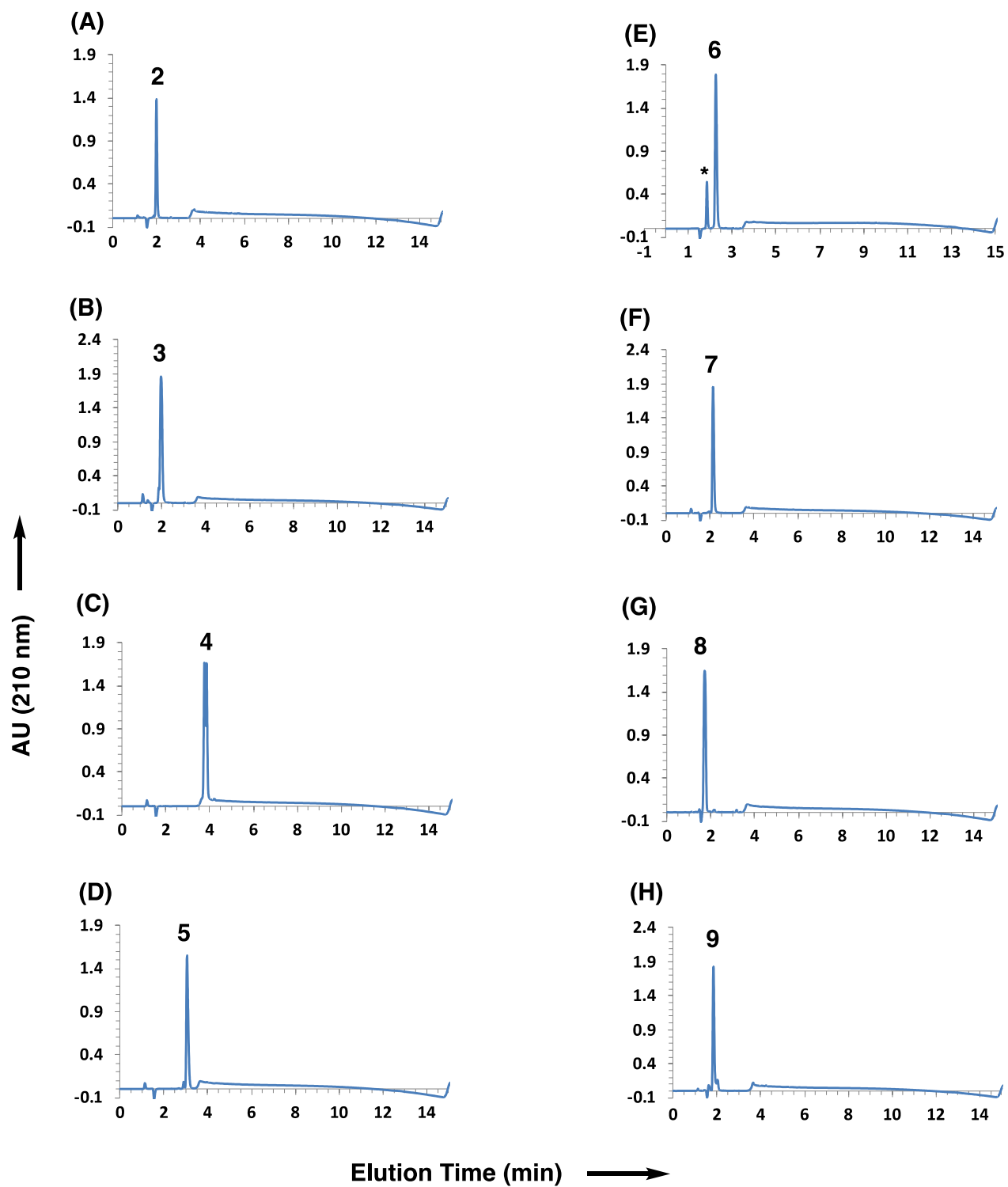


Figure S2. UPLC traces of oxime compounds **2** (A) to **9** (H). *denotes a void volume (solvent front) which runs closely overlapped with the compound peak.

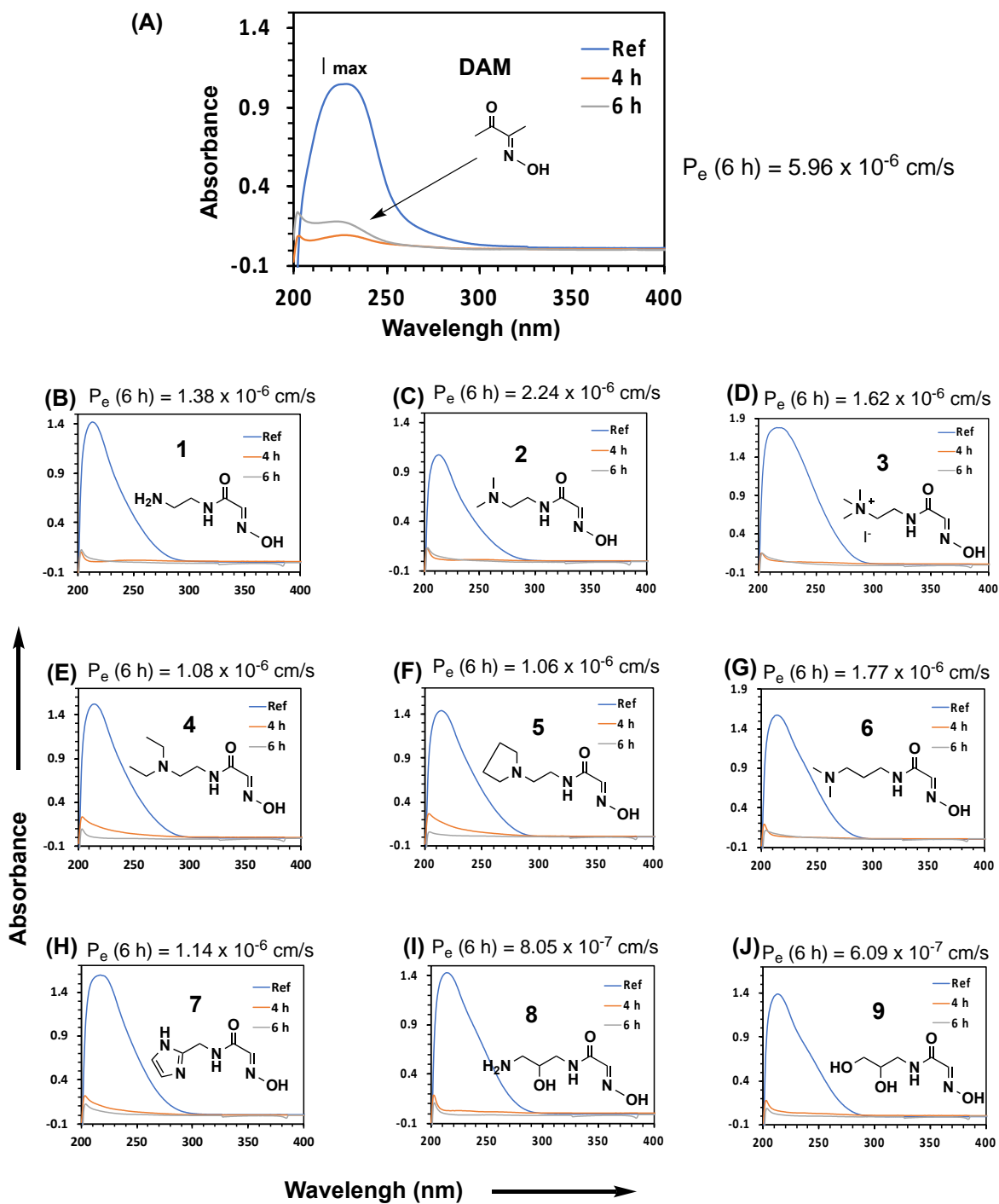


Figure S3. Overlaid UV-vis spectral traces of oximes **1–9** detected in acceptor wells from a parallel artificial membrane permeability assay (PAMPA)⁴ and values of their effective permeability (P_e). In this assay, each oxime solution (0.2 mM) in phosphate buffered saline pH 7.4 was loaded in donor wells and its rate of diffusion into the acceptor wells was assessed by absorbance (λ_{\max}) measured after incubation for a period of 4 h and 6 h. Each reference spectrum for an oxime compound drawn in blue was acquired at 67 μ M in the same buffer.

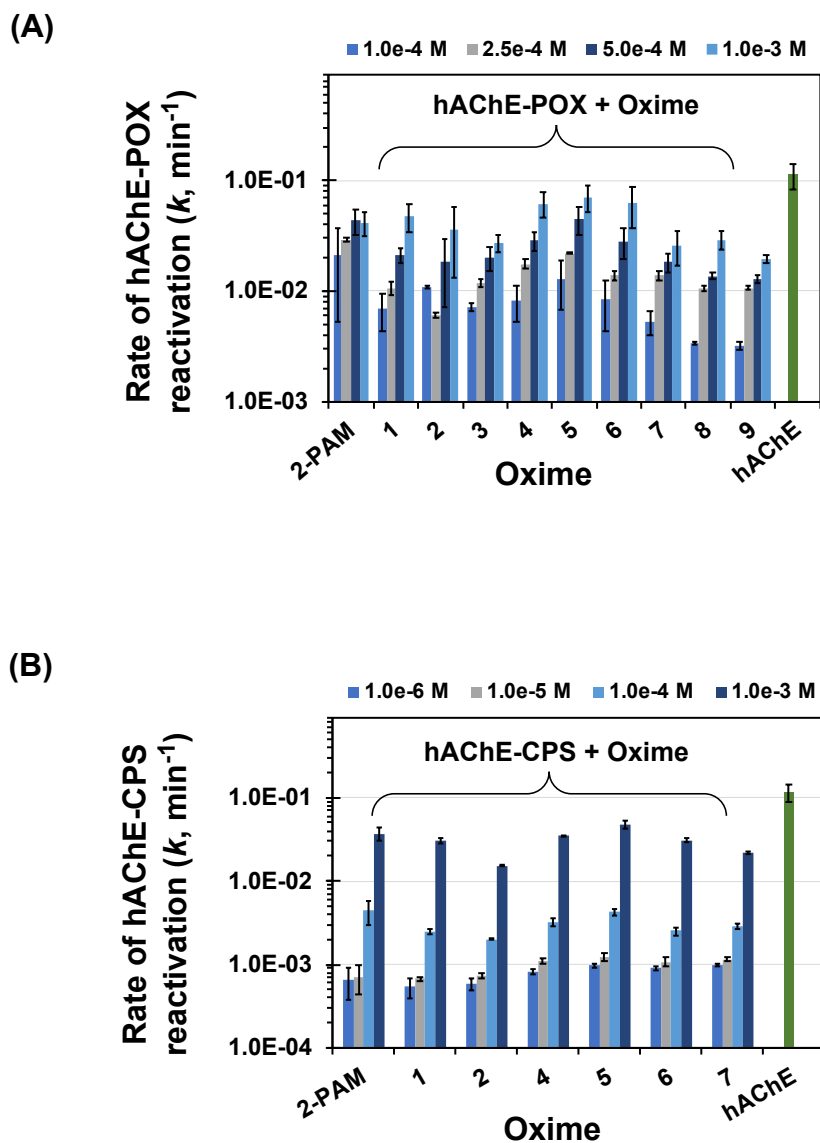


Figure S4. Plots of rate constant ($k = \Delta A_{412 \text{ nm}}/\Delta t$; min^{-1}) values for hAChE-POX (A) and hAChE-CPS (B) reactivation against oxime concentration. hAChE (0.2 U/mL) was pre-inhibited by POX (A) or CPS (B), each at 50 nM, prior to reactivation by oximes. Each value represents a mean \pm standard deviation (SD, $n = 3-6$).

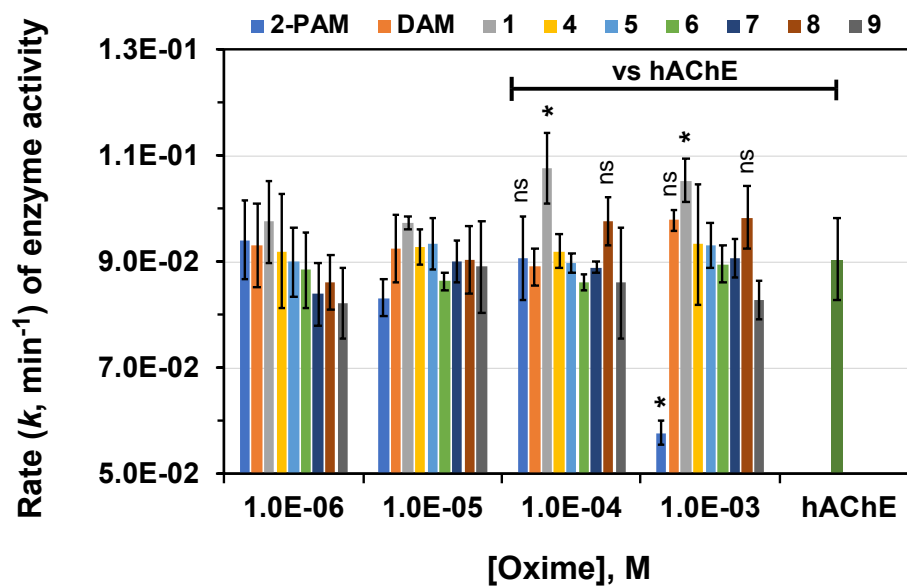


Figure S5. A plot of rate constant ($k = \Delta A_{412 \text{ nm}} / \Delta t$; min^{-1}) values for hAChE treated with oximes. hAChE (0.2 U/mL) was incubated with oximes **1**, **4–9** at variable oxime concentrations and its activity was measured in PBS pH 8.0, 17 ± 2 °C *in vitro*. Each value represents a mean \pm SD (n = 3–6). * p value < 0.05. ns = no significance ($p > 0.05$)

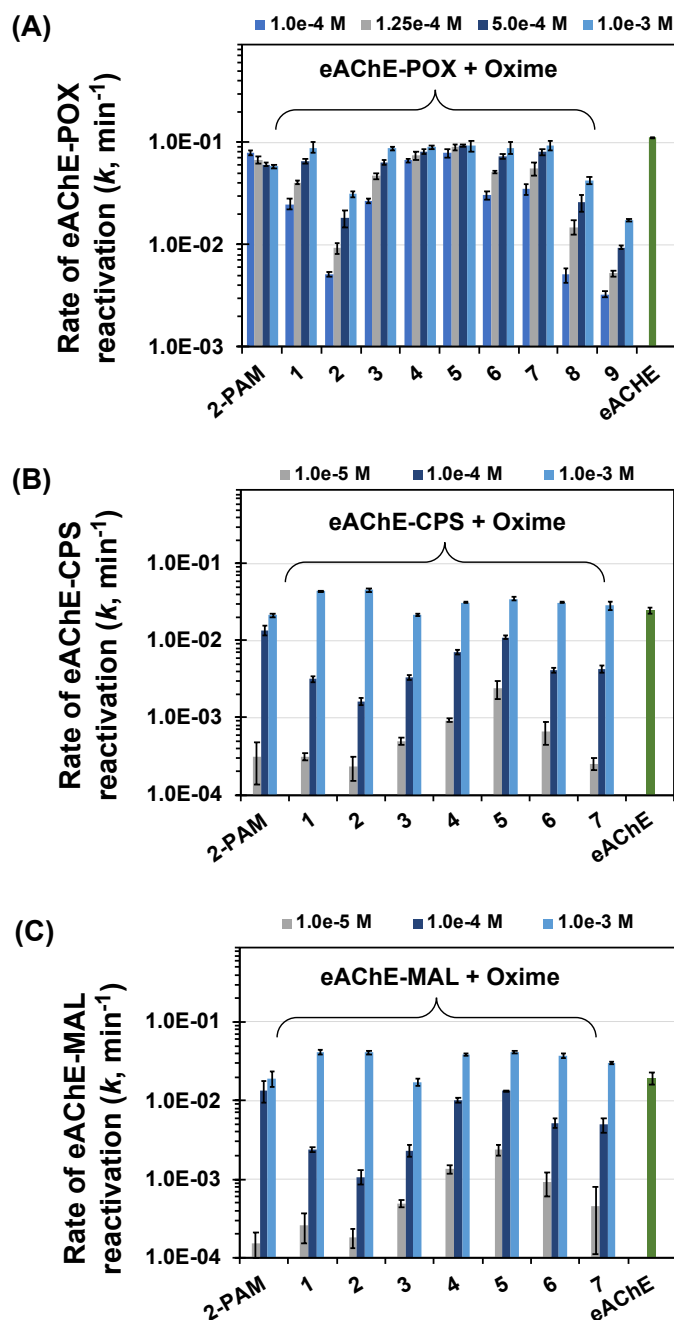


Figure S6. Plots of rate constant ($k = \Delta A_{412 \text{ nm}} / \Delta t; \text{min}^{-1}$) values for eAChE-POX (A), eAChE-CPS (B) and eAChE-MAL (C) reactivation against oxime concentration. eAChE (0.2 U/mL) was pre-inhibited by treatment with either POX (500 nM), CPS (50 nM) or MAL (250 nM) prior to reactivation by oximes. Each value represents a mean \pm SD ($n = 3-6$).

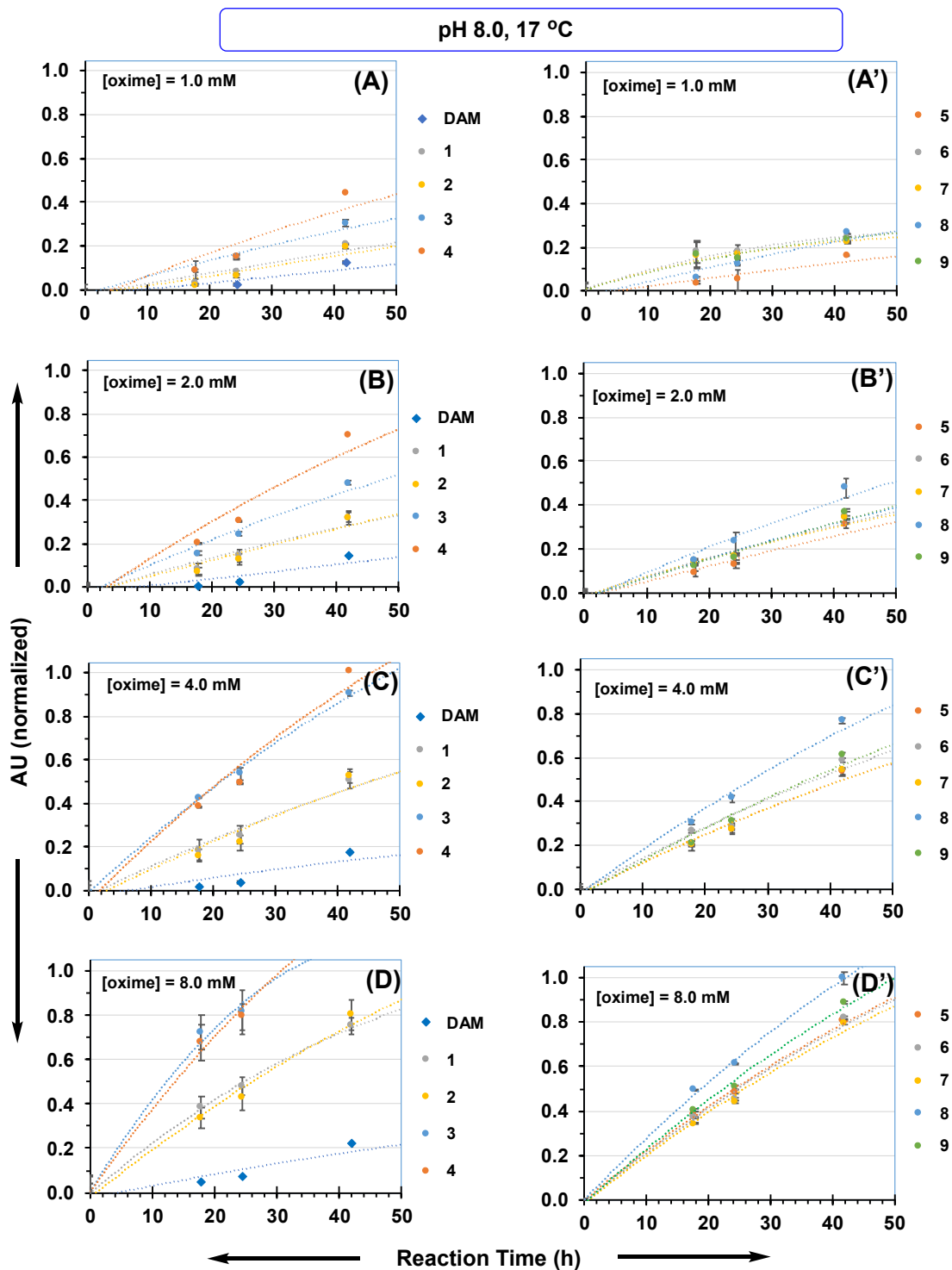


Figure S7. Kinetic traces of oxime-catalyzed POX inactivation in phosphate buffered saline pH 8.0, 17 ± 2 °C. POX (30 μ M) was incubated with each oxime formulated at 1.0 mM (A, A'), 2.0 mM (B, B'), 4.0 mM (C, C') or 8.0 mM (D, D'), and its inactivation progress was monitored by measuring absorbance at 400 nm (λ_{max} of 4-nitrophenol) as a function of time. Absorbance unit (AU) is normalized to a maximal level of absorbance (1.0 = full inactivation).

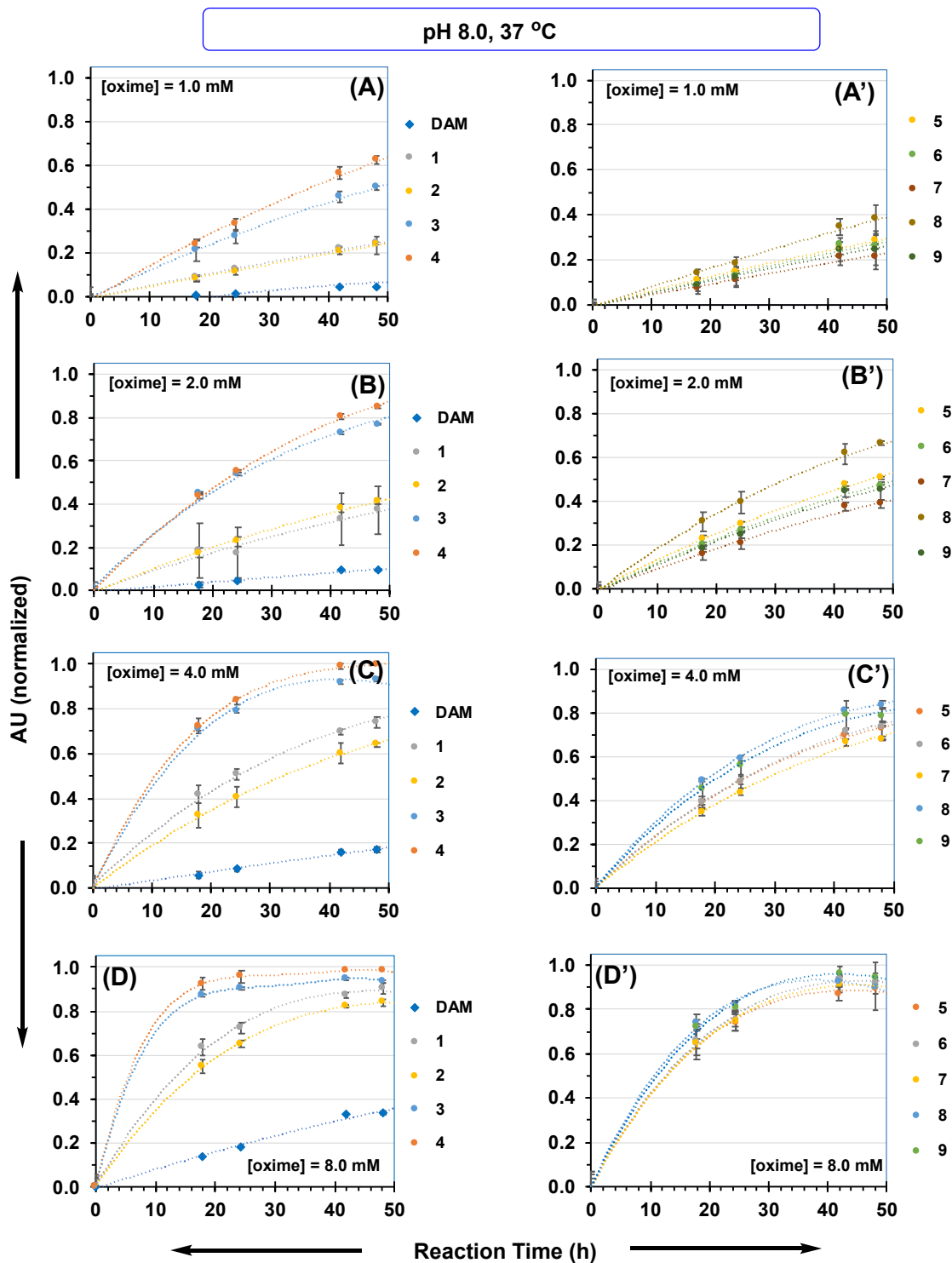


Figure S8. Kinetics of oxime-catalyzed POX inactivation at phosphate buffered saline pH 8.0, 37 ± 1 °C. POX (30 μ M) was incubated with each oxime formulated at 1.0 mM (A, A'), 2.0 mM (B, B'), 4.0 mM (C, C') and 8.0 mM (D, D'), and its inactivation progress was monitored by measuring an increase in absorbance at 400 nm (λ_{\max} of 4-nitrophenol) as a function of time. Absorbance unit (AU) is normalized to a maximal level of absorbance (1.0 = full inactivation).

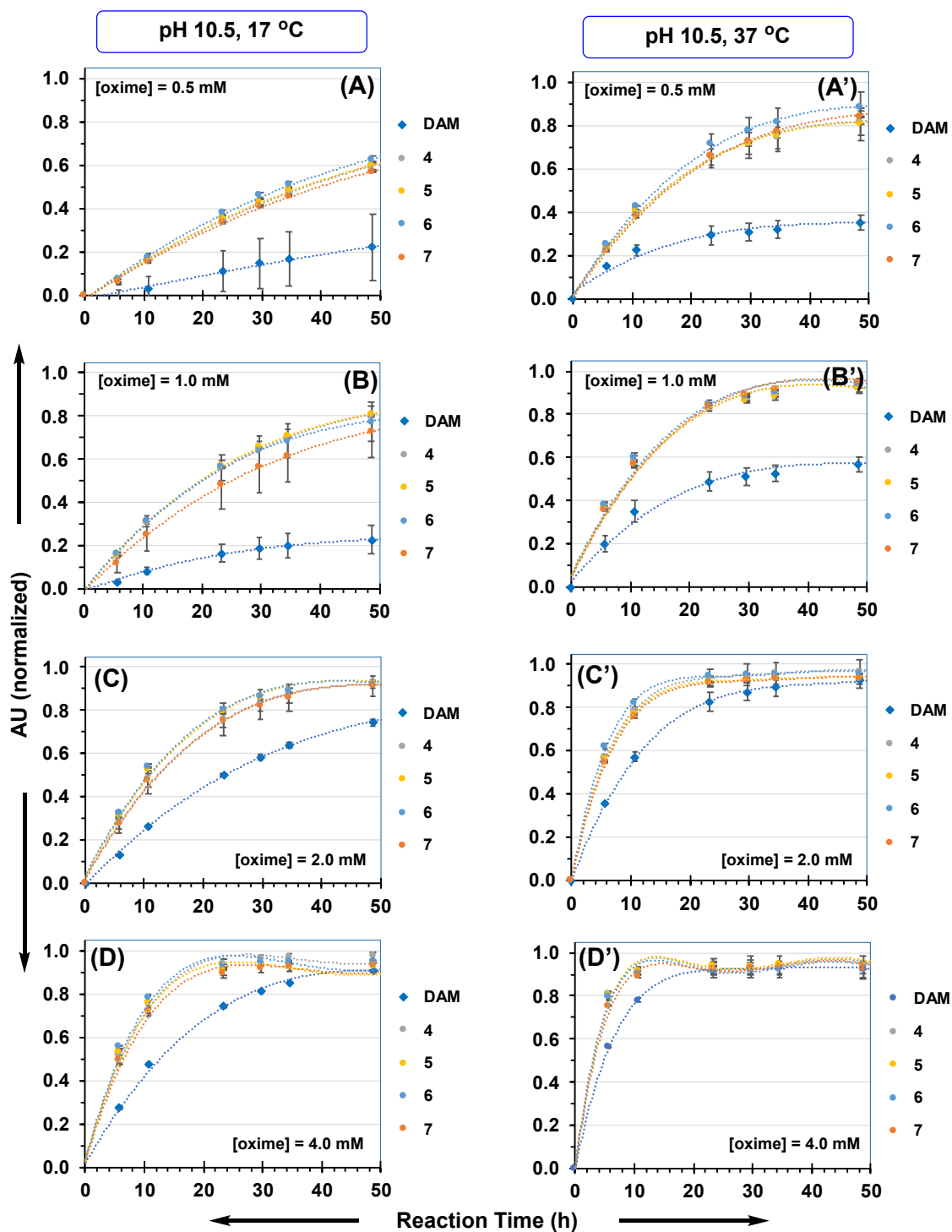


Figure S9. Kinetics of oxime-catalyzed POX inactivation at phosphate buffered saline pH 10.5, $37 \pm 1^\circ\text{C}$ or $17 \pm 2^\circ\text{C}$. POX ($30 \mu\text{M}$) was incubated with each oxime formulated at 0.5 mM (A, A'), 1.0 mM (B, B'), 2.0 mM (C, C') and 4.0 mM (D, D'), and its inactivation progress was monitored by measuring an increase in absorbance at 400 nm (λ_{max} of 4-nitrophenol) as a function of time. Absorbance unit (AU) is normalized to a maximal level of absorbance (1.0 = full inactivation).

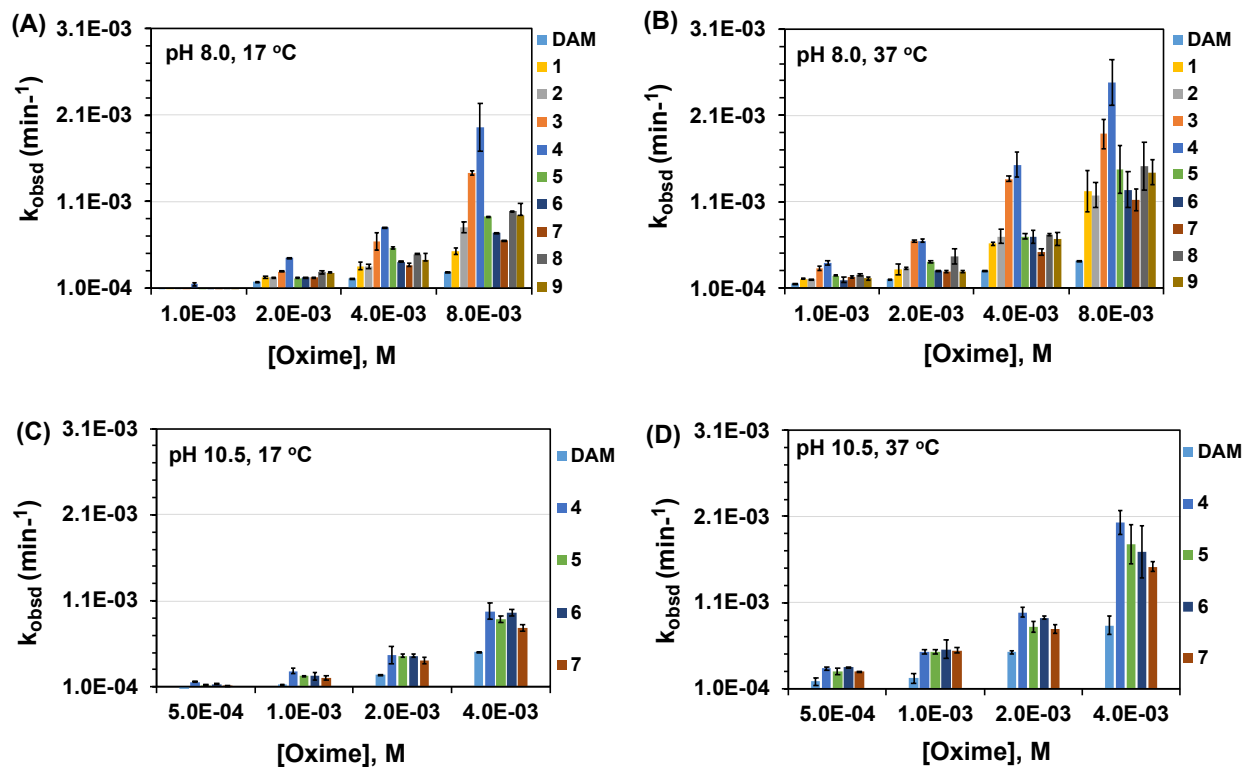


Figure S10. Plots of observed rate constant k_{obsd} (min⁻¹) determined from the kinetic traces of oxime-catalyzed POX inactivation as presented in Figures S7–S9. (A) pH 8.0, 17 ± 2 °C, (B) pH 8.0, 37 ± 1 °C ([Oxime] = 1.0–8.0 mM); (C) pH 10.5, 17 ± 2 °C, (D) pH 10.5, 37 ± 1 °C ([Oxime] = 0.5–4.0 mM). Each k value represents a mean \pm standard deviation ($n = 3$).

Table S1. Values of half-maximal inhibitory concentration (IC₅₀) of AChE by paraoxon (POX), chlorpyrifos (CPS), malaoxon (MAL) and omethoate (OME).

Enzyme		hAChE	eAChE
k ($\Delta A_{412 \text{ nm}}/\Delta t$), min ⁻¹		$8.67 (\pm 1.04) \times 10^{-2}$	$2.98 (\pm 0.16) \times 10^{-2}$
Normalized activity (%)		100 ± 9.9	100 ± 5.7
IC ₅₀ (nM)	POX	18 ± 1.3	51 ± 2.1
	CPS	8.0 ± 0.87	18 ± 1.1
	MAL	>1000	21 ± 4.3
	OME	>1000	>600

^a Each value refers to a mean \pm SD (n = 12 in k ; n = 3 in IC₅₀).

^b Abbreviations: hAChE = human recombinant AChE; eAChE = *Electrophorus electricus* AChE

References

1. Tang, S.; Wong, P. T.; Cannon, J.; Yang, K.; Bowden, S.; Bhattacharjee, S.; O'Konek, J. J.; Choi, S. K., Hydrophilic Scaffolds of Oxime as the Potent Catalytic Inactivator of Reactive Organophosphate. *Chem.-Biol. Interact.* **2019**, *297*, 67–79.
2. Wong, P.; Bhattacharjee, S.; Cannon, J.; Tang, S.; Yang, K.; Bowden, S.; Varnau, V.; O'Konek, J. J.; Choi, S. K., Reactivity and Mechanism of α -Nucleophile Scaffolds as Catalytic Organophosphate Scavengers. *Org. Biomol. Chem.* **2019**, *17* (16), 3951–3963.
3. Gündisch, D.; Andrä, M.; Munoz, L.; Cristina Tilotta, M., Synthesis and evaluation of phenylcarbamate derivatives as ligands for nicotinic acetylcholine receptors. *Bioorg. Med. Chem.* **2004**, *12* (18), 4953–4962.
4. Yu, H.; Wang, Q.; Sun, Y.; Shen, M.; Li, H.; Duan, Y., A New PAMPA Model Proposed on the Basis of a Synthetic Phospholipid Membrane. *PLoS One* **2015**, *10* (2), e0116502.
5. Liu, H.; Sabus, C.; Carter, G. T.; Du, C.; Avdeef, A.; Tischler, M., In Vitro Permeability of Poorly Aqueous Soluble Compounds Using Different Solubilizers in the PAMPA Assay with Liquid Chromatography/Mass Spectrometry Detection. *Pharm. Res.* **2003**, *20* (11), 1820–1826.
6. Ellman, G. L.; Courtney, K. D.; Andres jr, V.; Featherstone, R. M., A New and Rapid Colorimetric Determination of Acetylcholinesterase Activity. *Biochem. Pharmacol. (Amsterdam, Neth.)* **1961**, *7* (2), 88–95.
7. Cochran, R.; Kalisiak, J.; Küçükılınç, T.; Radić, Z.; Garcia, E.; Zhang, L.; Ho, K.-Y.; Amitai, G.; Kovarik, Z.; Fokin, V. V.; Sharpless, K. B.; Taylor, P., Oxime-assisted Acetylcholinesterase Catalytic Scavengers of Organophosphates That Resist Aging. *J. Biol. Chem.* **2011**, *286* (34), 29718–29724.
8. de Koning, M. C.; Horn, G.; Worek, F.; van Grol, M., Discovery of a potent non-oxime reactivator of nerve agent inhibited human acetylcholinesterase. *Eur. J. Med. Chem.* **2018**, *157*, 151–160.
9. Garcia, G. E.; Campbell, A. J.; Olson, J.; Moorad-Doctor, D.; Morthole, V. I., Novel oximes as blood–brain barrier penetrating cholinesterase reactivators. *Chem.-Biol. Interact.* **2010**, *187* (1–3), 199–206.
10. Bharathi, S.; Wong, P. T.; Desai, A.; Lykhytska, O.; Choe, V.; Kim, H.; Thomas, T. P.; Baker, J. R.; Choi, S. K., Design and Mechanistic Investigation of Oxime-conjugated PAMAM Dendrimers As the Catalytic Scavenger of Reactive Organophosphate. *J. Mater. Chem. B* **2014**, *2* (8), 1068–1078.
11. Wong, P. T.; Tang, S.; Cannon, J.; Yang, K.; Harrison, R.; Ruge, M.; O'Konek, J. J.; Choi, S. K., Shielded α -Nucleophile Nanoreactor for Topical Decontamination of Reactive Organophosphate. *ACS Appl. Mater. Interfaces* **2020**, *12* (30), 33500–33515.